[Supplementary material]

The integration of millet into the diet of Central Asian populations in the third millennium BC

Giedre Motuzaite Matuzeviciute[1,*][ORCID: 0000-0001-9069-1551], Elina Ananyevskaya[1], Jorune Sakalauskaite[2][ORCID: 0000-0002-8029-8120], Orozbek Soltobaev[3] & Kubatbek Tabaldiev[4][ORCID: 0000-0002-6679-8030]

[1] Department of Archaeology, Vilnius University, Lithuania

[2] Department of Life Sciences and Systems Biology, University of Turin, Italy

[3] Department of Archaeology and Ethnography, Kyrgyz National University, Bishkek, Kyrgyzstan

[4] Department of Archaeology, Kyrgyz-Turkish Manas University, Bishkek, Kyrgyzstan

[*] Author for correspondence ✉ giedre.motuzaite@gmail.com

OSM A

Table S1a. $\delta^{13}C$ and $\delta^{15}N$ values of human remains from Kyrgyzstan.

Lab number	Site	Context	Element	Period	$\delta^{13}C$	$\delta^{15}N$	N%	C%	C/N atomic
BTC-KY-H1	Aigyrzhal 1	od. 3	Human petrous	Early–Late BA (2500–1200 BC)	−18.48	11.99	19.53	53.02	3.2
BTC-KY-H2	Aigyrzhal 1	K. 60 child	Human petrous	Early–Late BA (2500–1200 BC)	−18.20	14.01	18.49	49.57	3.1
BTC-KY-H3	Aigyrzhal 1	od. 2	Human petrous	Early–Late BA (2500–1200 BC)	−18.82	11.86	19.38	51.62	3.1
BTC-KY-H4	Aigyrzhal 1	K. 55	Human petrous	Early–Late BA (2500–1200 BC)	−17.90	12.07	15.90	43.85	3.2
BTC-KY-H5	Aigyrzhal 1	K. 11	Human petrous	Early–Late BA (2500–1200 BC)	−18.62	16.90	20.82	56.98	3.2
BTC-KY-H6	Aigyrzhal 1	K. 60 adult	Human petrous	Early–Late BA (2500–1200 BC)	−17.16	11.62	17.07	45.64	3.1
BTC-KY-H7	Aigyrzhal 1	K. 125	Human petrous	Early–Late BA (2500–1200 BC)	−17.88	12.28	14.86	41.01	3.2
BTC-KY-H24	Aigyrzhal 2		Human petrous	Early–Late BA (2500–1200 BC)	−17.62	11.72	13.98	37.02	3.1
BTC-KY-H25	Aigyrzhal 2		Human petrous	Early–Late BA (2500–1200 BC)	−17.80	11.80	14.40	38.29	3.1
BTC-KY-H26	Aigyrzhal 2		Human petrous	Early–Late BA (2500–1200 BC)	−18.80	11.00	15.28	40.63	3.1

BTC-KY-H27	Aigyrzhal 2		Human petrous	Early–Late BA (2500–1200 BC)	−18.25	12.54	13.31	36.54	3.2
BTC-KY-H28	Aigyrzhal 2		Human petrous	Early–Late BA (2500–1200 BC)	−18.80	11.10	14.80	39.87	3.1
BTC-KY-H29	Aigyrzhal 2		Human petrous	Early–Late BA (2500–1200 BC)	−17.61	11.73	14.56	38.87	3.1
BTC-KY-H30	Aigyrzhal 2	K. 19	Human petrous	Early–Late BA (2500–1200 BC)	−18.73	12.28	17.09	46.70	3.2
BTC-KY-H36	Aigyrzhal 2	Kurgan 135	Human metapodia	Early–Late BA (2500–1200 BC)	−18.08	10.50	12.97	33.95	3.1
BTC-KY-H37	Aigyrzhal 3		Human metapodia	Early–Late BA (2500–1200 BC)	−18.00	11.10	14.36	38.05	3.1
BTC-KY-H38	Aigyrzhal 3	od. 1	Human petrous	Early–Late BA (2500–1200 BC)	−18.83	12.72	18.90	51.52	3.2
BTC-KY-H39	Aigyrzhal 3	Object 1, burial 20	Child vertebra	Early–Late BA (2500–1200 BC)	−18.74	13.82	20.24	54.03	3.1
BTC-KY-H40	Aigyrzhal 3	Object 1, burial 5	Child vertebra	Early–Late BA (2500–1200 BC)	−18.80	13.80	16.24	42.66	3.1
BTC-KY-H41	Aigyrzhal 3	Object 1, burial 7	Child vertebra	Early–Late BA (2500–1200 BC)	−18.78	13.66	21.20	56.13	3.1
BTC-KY-H42	Aigyrzhal 3	Object 1, burial 16	Child vertebra	Early–Late BA (2500–1200 BC)	−18.55	11.79	18.08	47.08	3.0
BTC-KY-H43	Aigyrzhal 3	Object 1, burial 5	Child vertebra	Early–Late BA (2500–1200 BC)	−19.34	11.18	17.53	46.28	3.1
BTC-KY-H44	Aigyrzhal 3	Object 1, burial 13	Child vertebra	Early–Late BA (2500–1200 BC)	−19.18	12.80	16.60	43.49	3.1
BTC-KY-H45	Aigyrzhal 3	Object 1, burial 14	Child vertebra	Early–Late BA (2500–1200 BC)	−19.05	12.56	17.14	44.69	3.0
BTC-KY-H46	Aigyrzhal 3	Kurgan 2, burial 4	Human metapodia	Early–Late BA (2500–1200 BC)	−19.43	10.10	23.07	59.58	3.0
BTC-KY-H47	Aigyrzhal 3	Kurgan 137	Human skull	Early–Late BA (2500–1200 BC)	−18.17	11.14	13.45	34.87	3.0
BTC-KY-H48	Aigyrzhal 3	Kurgan 139	Human skull	Early–Late BA (2500–1200 BC)	−12.34	10.88	7.03	18.93	3.1
BTC-KY-H49	Aigyrzhal 3	Object 1, Ograda 23	Child vertebra	Early–Late BA (2500–1200 BC)	−18.74	13.19	16.59	43.34	3.0
BTC-KY-H50	Aigyrzhal 3	Object 1, Ograda 16	Child metapodia	Early–Late BA (2500–1200 BC)	−18.78	11.50	18.10	46.48	3.0
BTC-KY-H51	Aigyrzhal 3	Object 1, ograda 3	Child vertebra	Early–Late BA (2500–1200 BC)	−18.51	12.30	20.45	53.97	3.1
BTC-KY-H52	Aigyrzhal 3	Object 1, ograda 17	Juvenile <16 y.o. 1st phalanx	Early–Late BA (2500–1200 BC)	−19.18	11.25	13.56	35.05	3.0

BTC-KY-H53	Aigyrzhal 3	Object 3, ograda 2	Child vertebra	Early–Late BA (2500–1200 BC)	−19.18	10.26	16.47	43.19	3.1
BTC-KY-H54	Aigyrzhal 3	Object 1, ograda 22	Child clavicle	Early–Late BA (2500–1200 BC)	−19.19	11.64	12.46	32.62	3.1
BTC-KY-H55	Aigyrzhal 3	Object 1, ograda 18	Juvenile <16 y.o. 1st phalanx	Early–Late BA (2500–1200 BC)	−18.52	11.55	23.81	61.64	3.0
BTC-KY-H56	Aigyrzhal 3	Object 1, ograda 21	Child skull	Early–Late BA (2500–1200 BC)	−19.20	12.73	10.86	29.34	3.2
BTC-KY-H57	Aigyrzhal 3	Object 1, ograda 4	Child vertebra	Early–Late BA (2500–1200 BC)	−19.09	12.71	14.57	38.33	3.1
BTC-KY-H58	Chalchyk-Bulak	kurgan 1	Skull bone	Early–Late BA (2500–1200 BC)	−18.33	12.48	n/k	n/k	3.1
BTC-KY-H66	Kara-Tumshuk		Childs burial/Koch-kor valley	Early–Late BA (2500–1200 BC)	−18.40	11.9	13.87	37.3	3.1
BTC-KY-H67	Kochkor burial grounds	plundered burial	Human	Early–Late BA (2500–1200 BC)	−18.71	12.72	13.43	37.05	3.2
BTC-KY-H69	Kyrk-Sheyit	3rd skeleton	Human skull	Early–Late BA (2500–1200 BC)	−18.31	12.34	17.27	45.02	3.0
BTC-KY-H70	Kyrk-Sheyit	2nd skeleton	Human skull	Early–Late BA (2500–1200 BC)	−19.18	10.72	16.81	43.65	3.0
BTC-KY-H71	Kyrk-Sheyit	1st skeleton	Human skull	Early–Late BA (2500–1200 BC)	−18.66	9.97	9.52	25.02	3.1
BTC-KY-H74	Shyldyrak	Ogradka 3	Human 2nd phalanx	Early–Late BA (2500–1200 BC)	−16.91	11.53	14.13	37.14	3.1
BTC-KY-H75	Shyldyrak	Ogradka 1	Vertebra	Early–Late BA (2500–1200 BC)	−17.23	11.04	8.38	22.86	3.2
BTC-KY-H76	Shyldyrak	Ogradka 4	Human 1st phalanx	Early–Late BA (2500–1200 BC)	−18.34	10.99	20.35	52.63	3.0
BTC-KY-H79	Chap II	2020 excavation	Human rib	Early–Late BA (2500–1200 BC)	−17.45	12.67	15.18	42.58	3.3
BTC-KY-H77	Uch-Kurbu	kurgan 6		Final BA – EIA (1200–200 BC)	−17.04	11.80	13.45	35.88	3.1
BTC-KY-H15	Aigyrzhal 1	K. 4	Human petrous	Final BA – EIA (1200–200 BC)	−17.87	13.27	18.53	51.12	3.2
BTC-KY-H18	Aigyrzhal 1	K. 7, n. 2	Human petrous	Final BA – EIA (1200–200 BC)	−15.62	12.74	17.08	46.31	3.2
BTC-KY-H19	Aigyrzhal 1	K. 28	Human petrous	Final BA – EIA (1200–200 BC)	−18.47	12.67	18.98	50.72	3.1

BTC-KY-H22	Aigyrzhal 1	K. 8	Human petrous	Final BA – EIA (1200–200 BC)	−17.90	11.60	18.29	49.47	3.2
BTC-KY-H31	Aigyrzhal 2	K. 10	Human petrous	Final BA – EIA (1200–200 BC)	−14.46	13.05	17.29	46.42	3.1
BTC-KY-H32	Aigyrzhal 2			Final BA – EIA (1200–200 BC)	−17.50	12.50	15.58	41.34	3.1
BTC-KY-H33	Aigyrzhal 2			Final BA – EIA (1200–200 BC)	−17.90	12.20	14.74	39.51	3.1
BTC-KY-H34	Aigyrzhal 2			Final BA – EIA (1200–200 BC)	−17.81	12.08	14.73	39.04	3.1
BTC-KY-H35	Aigyrzhal 2			Final BA – EIA (1200–200 BC)	−17.72	12.83	14.73	39.29	3.1
BTC-KY-H60	Chap I	2002-2003 excav.	Human skull	Final BA – EIA (1200–200 BC)	−13.92	12.23	15.02	41.64	3.2
BTC-KY-H61	Chap I	Burial 1 in 2018 exc.	Human rib	Final BA – EIA (1200–200 BC)	−18.71	11.52	11.22	31.69	3.3
BTC-KY-H62	Chap I	C 118, C2, 7Aug	Human phalanx	Final BA – EIA (1200–200 BC)	−18.42	11.34	13.82	39.03	3.3
BTC-KY-H63	Chechen-Bulak	Kurgan 1	Human first phalanx	Final BA – EIA (1200–200 BC)	−16.90	9.99	17.92	46.64	3.0
BTC-KY-H64	Chon-Alai	Kurgan 1, intrusive burial	Human vertebra	Final BA – EIA (1200–200 BC)	−17.15	11.43	11.96	31.67	3.1
BTC-KY-H65	Chon-Alai	Kurgan 1	Human vertebra	Final BA – EIA (1200–200 BC)	−17.73	10.70	12.69	33.20	3.1
BTC-KY-H72	Mechet at-Bashi			Final BA – EIA (1200–200 BC)	−18.71	12.92	15.36	41.41	3.1
BTC-KY-H73	Mechet at-Bashi			Final BA – EIA (1200–200 BC)	−18.12	12.93	15.64	42.22	3.1
BTC-KY-H78	Zhapyryk			Final BA – EIA (1200–200 BC)	−15.74	12.11	15.51	41.79	3.1
BTC-KY-H8	Aigyrzhal 1	K. 2	Human petrous	Turkic–Medieval (200 BC – AD 1700)	−18.56	13.26	16.54	44.60	3.1
BTC-KY-H9	Aigyrzhal 1	K. 24a	Human petrous	Turkic–Medieval (200 BC – AD 1700)	−18.28	12.89	18.99	52.01	3.2
BTC-KY-H10	Aigyrzhal 1	K. 120	Human petrous	Turkic–Medieval (200 BC – AD 1700)	−17.84	12.53	22.44	60.58	3.1
BTC-KY-H11	Aigyrzhal 1	K. 7, n. 3	Human petrous	Turkic–Medieval (200 BC – AD 1700)	−18.22	12.34	18.27	49.26	3.1
BTC-KY-H12	Aigyrzhal 1	K. 7, n. 1	Human petrous	Turkic–Medieval (200 BC – AD 1700)	−15.61	13.16	18.33	50.00	3.2

BTC-KY-H13	Aigyrzhal 1	K. 1	Human petrous	Turkic–Medieval (200 BC – AD 1700)	−15.33	13.29	10.49	29.97	3.3
BTC-KY-H14	Aigyrzhal 1	K. 20	Human petrous	Turkic–Medieval (200 BC – AD 1700)	−18.47	12.57	19.23	52.24	3.2
BTC-KY-H16	Aigyrzhal 1	K. 14	Human petrous	Turkic–Medieval (200 BC – AD 1700)	−18.29	17.31	15.29	42.44	3.2
BTC-KY-H17	Aigyrzhal 1	K. 24ab	Human petrous	Turkic–Medieval (200 BC – AD 1700)	−18.65	12.57	21.06	57.21	3.2
BTC-KY-H20	Aigyrzhal 1	K. 45	Human petrous	Turkic–Medieval (200 BC – AD 1700)	−19.92	15.20	18.97	49.52	3.0
BTC-KY-H21	Aigyrzhal 1	K. 50	Human petrous	Turkic–Medieval (200 BC – AD 1700)	−18.01	11.72	18.96	52.12	3.2
BTC-KY-H23	Aigyrzhal 1	K. 47	Human petrous	Turkic–Medieval (200 BC – AD 1700)	−18.55	12.39	12.88	35.08	3.2
BTC-KY-H68	Kok-Tash		Rib	Turkic–Medieval (200 BC–AD 1700)	−16.91	13.80	10.19	29.45	3.4

Table S1b. $\delta^{13}C$ and $\delta^{15}N$ values of faunal remains from Kyrgyzstan.

Lab number	**Site**	**Context**	**Species**	**Element**	**Dating**	**$\delta^{13}C$‰**	**$\delta^{15}N$‰**	**N%**	**C%**	**C/N**
BTC-KY-F6	Aigyrzhal 1	Sack 1, individual 1	Horse	Carpus/tarsus	Early–Late BA (2500–1200 BC)	–20.51	6.33	21.45	56.02	3.0
BTC-KY-F8	Aigyrzhal 1	Kurgan 18	Horse	Splinter	Early–Late BA (2500–1200 BC)	–20.53	5.59	16.55	42.87	3.0
BTC-KY-F7	Aigyrzhal 2	Kurgan 24	Horse	Cuboid	Early–Late BA (2500–1200 BC)	–20.62	5.22	12.37	33.19	3.1
BTC-KY-F10	Aigyrzhal 2	Kurgan 9	Horse	Carpus/tarsus	Early–Late BA (2500–1200 BC)	–19.99	5.30	12.53	32.85	3.1
BTC-KY-F11	Aigyrzhal 2	Kurgan 28	Horse	Cuboid	Early–Late BA (2500–1200 BC)	–20.72	5.66	20.75	53.81	3.0
BTC-KY-F14	Aigyrzhal 2	Kurgan 24A	Horse	Cuboid	Early–Late BA (2500–1200 BC)	–20.23	5.63	20.55	53.37	3.0
BTC-KY-F16	Aigyrzhal 2	Kurgan 184	Caprine	Radius	Early–Late BA (2500–1200 BC)	–18.63	7.04	24.87	64.13	3.0

BTC–KY–F17	Aigyrzhal 2	Kurgan 184	Caprine	Lower jaw	Early–Late BA (2500–1200 BC)	–19.21	6.41	11.97	32.24	3.1
BTC–KY–F18	Aigyrzhal 2	Kurgan 184	Horse	Scapula	Early–Late BA (2500–1200 BC)	–20.53	4.97	17.30	45.15	3.0
BTC–KY–F19	Aigyrzhal 2	Kurgan 184	Wild goat	Horncore	Early–Late BA (2500–1200 BC)	–18.87	4.90	16.00	42.31	3.1
BTC–KY–F52	Aigyrzhal 2	BA	Big mammal (horse, cattle, etc.)	Bone fragment	Early–Late BA (2500–1200 BC)	–19.52	6.91	14, 90	39.68	3.1
BTC–KY–F53	Aigyrzhal 2	BA	Caprine	Bone fragment	Early–Late BA (2500–1200 BC)	–19.22	5.51	14.18	37.87	3.1
BTC–KY–F56	Aigyrzhal 2	MBA (1700 BC)	Caprine	Bone fragment	Early–Late BA (2500–1200 BC)	–19.75	7.12	n/k	n/k	3.2
BTC–KY–F9	Aigyrzhal 3	Kurgan 137	Caprine	Rib	Early–Late BA (2500–1200 BC)	–18.82	5.89	8.10	22.24	3.2
BTC–KY–F34	Chap II	C2.3D	Capra	Bone fragment	Early–Late BA (2500–1200 BC)	–19.35	8.38	41.26	14.98	3.2
BTC–KY–F35	Chap II	C2.3D	Bos	Bone fragment	Early–Late BA (2500–1200 BC)	–18.76	7.22	43.50	15.83	3.2
BTC–KY–F36	Chap II	C2.3D	Bos	Bone fragment	Early–Late BA (2500–1200 BC)	–19.04	6.57	43.66	15.96	3.2
BTC–KY–F37	Chap II	C2.3B	Ovis	Bone fragment	Early–Late BA (2500–1200 BC)	–19.46	6.99	45.24	16.48	3.2
BTC–KY–F38	Chap II	C2.4.1G	Bos	Bone fragment	Early–Late BA (2500–1200 BC)	–19.40	8.66	46.08	16.68	3.2
BTC–KY–F39	Chap II	C2.4.1G	Bos	Bone fragment	Early–Late BA (2500–1200 BC)	–19.11	7.00	39.14	14.19	3.2
BTC–KY–F40	Chap II	C2.4.1G	Ovis	Bone fragment	Early–Late BA (2500–1200 BC)	–18.99	7.66	44.68	16.32	3.2
BTC–KY–F41	Chap II	C2.4.1G	Bos	Bone fragment	Early–Late BA (2500–1200 BC)	–18.88	6.97	38.37	13.84	3.2
BTC–KY–F42	Chap II	C2.4.1G	Bos	Bone fragment	Early–Late BA (2500–1200 BC)	–18.92	7.69	39.17	14.28	3.2
BTC–KY–F43	Chap II	C2.4.1G	Ovis	Bone fragment	Early–Late BA (2500–1200 BC)	–19.73	8.11	38.13	13.74	3.2
BTC–KY–F44	Chap II	C2.2C	Ovis	Bone fragment	Early–Late BA (2500–1200 BC)	–19.08	6.93	46.20	16.62	3.2
BTC–KY–F45	Chap II	C2.2C	Bos	Bone fragment	Early–Late BA (2500–1200 BC)	–15.99	7.78	39.15	13.75	3.3

BTC–KY–F46	Chap II	C2.1F	Ovis	Bone fragment	Early–Late BA (2500–1200 BC)	–18.82	5.78	41.74	15.08	3.2
BTC–KY–F47	Chap II	C2.1F	Bos	Bone fragment	Early–Late BA (2500–1200 BC)	–18.55	7.53	41.12	14.90	3.2
BTC–KY–F48	Chap II	C2.1F	Bos	Bone fragment	Early–Late BA (2500–1200 BC)	–18.71	6.98	44.58	16.29	3.2
BTC–KY–F49	Chap II	C2.1F	Bos	Bone fragment	Early–Late BA (2500–1200 BC)	–19.20	7.28	32.23	11.21	3.4
BTC–KY–F50	Chap II	C2.1F	Bos	Bone fragment	Early–Late BA (2500–1200 BC)	–18.70	6.99	43.60	15.73	3.2
BTC–KY–F51	Chap II	C2.1F	Bos	Bone fragment	Early–Late BA (2500–1200 BC)	–19.03	8.08	37.80	13.50	3.3
BTC–KY–F1	Kara–Tumshuk	Ky19.8F, part of human burial	Caprine	Cervical vertebra	Early–Late BA (2500–1200 BC)	–20.24	6.69	42.24	14.99	3.3
BTC–KY–F2	Kara–Tumshuk	human burial	cf. Horse	Bone fragment	Early–Late BA (2500–1200 BC)	–17.09	7.82	35.35	12.90	3.2
BTC–KY–F3	Kara–Tumshuk	KY19.7.F, part of human burial, 0.3m depth	Horse	Bone fragment	Early–Late BA (2500–1200 BC)	–20.87	4.19	30.60	10.94	3.3
BTC–KY–F4	Kara–Tumshuk	KY19.5.F	Caprine	Scapula	Early–Late BA (2500–1200 BC)	–17.98	7.19	34.82	12.08	3.4
BTC–KY–F5	Kara–Tumshuk	Ky19.2	Caprine	Carpus/tarsus	Early–Late BA (2500–1200 BC)	–18.71	11.23	36.45	13.00	3.3
BTC–KY–F80	Chap II	2020 excavation	cf. Cattle	Bone fragment	Early–Late BA (2500–1200 BC)	–19.30	8.07	14.33	42.01	3.5
BTC–KY–F81	Chap II	2020 excavation	Cattle	Bone fragment	Early–Late BA (2500–1200 BC)	–19.25	8.22	15.03	42.55	3.3
BTC–KY–F82	Chap II	2020 excavation	Animal	Bone fragment	Early–Late BA (2500–1200 BC)	–19.69	9.73	10.44	30.74	3.3
BTC–KY–F83	Chap II	2020 excavation	cf. Cattle	Bone fragment	Early–Late BA (2500–1200 BC)	–19.00	9.72	15.53	43.96	3.4
BTC–KY–F84	Chap II	2020 excavation	Sheep	Bone fragment	Early–Late BA (2500–1200 BC)	–18.41	6.98	14.49	41.10	3.3
BTC–KY–F85	Chap II	2020 excavation	cf. Cattle	Bone fragment	Early–Late BA (2500–1200 BC)	–19.68	8.30	13.17	38.44	3.4
BTC–KY–F86	Chap II	2020 excavation	Sheep	Bone fragment	Early–Late BA (2500–1200 BC)	–19.10	9.74	14.87	42.22	3.3

BTC–KY–F87	Chap II	2020 excavation	Sheep	Bone fragment	Early–Late BA (2500–1200 BC)	–19.51	10.63	15.14	42.82	3.3
BTC–KY–F88	Chap II	2020 excavation	Sheep	Bone fragment	Early–Late BA (2500–1200 BC)	–19.24	9.24	14.54	40.99	3.3
BTC–KY–F89	Chap II	2020 excavation	Horse	Bone fragment	Early–Late BA (2500–1200 BC)	–21.10	5.43	14.39	40.59	3.3
BTC–KY–F90	Chap II	2020 excavation	Cattle	Bone fragment	Early–Late BA (2500–1200 BC)	–17.76	7.41	14.71	41.58	3.3
BTC–KY–F91	Chap II	2020 excavation	Sheep	Bone fragment	Early–Late BA (2500–1200 BC)	–18.57	7.51	15.85	44.97	3.3
BTC–KY–F92	Chap II	2020 excavation	Sheep	Bone fragment	Early–Late BA (2500–1200 BC)	–18.56	7.15	15.38	43.46	3.3
BTC–KY–F93	Chap II	2020 excavation	Sheep	Bone fragment	Early–Late BA (2500–1200 BC)	–16.68	8.24	14.45	41.38	3.3
BTC–KY–F94	Chap II	2020 excavation	Sheep	Bone fragment	Early–Late BA (2500–1200 BC)	–19.82	6.57	5.30	15.62	3.5
BTC–KY–F65	Aigyrzhal 2	Saka/wusun people	Caprine	Bone fragment	Final BA/EIA (1200–200 BC)	–18.19	7.05	15.29	40.67	3.1
BTC–KY–F73	Chap I	C 114, sq. 2G	Caprine	Proximal metacarpal	Final BA/EIA (1200–200 BC)	–19.39	7.53	19.07	51.62	3.2
BTC–KY–F74	Chap I	C 105, B 1005, sq. F–E/6–7	Caprine	Proximal femur	Final BA/EIA (1200–200 BC)	–18.88	7.21	16.22	44.31	3.2
BTC–KY–F75	Chap I	C 114, B 1046, sq. 5D	Caprine	Ulna	Final BA/EIA (1200–200 BC)	–19.10	6.77	20.51	55.26	3.1
BTC–KY–F76	Chap I	C 133, lower levels	Caprine	Lower jaw	Final BA/EIA (1200–200 BC)	–19.52	6.66	19.01	53.56	3.3
BTC–KY–F77	Chap I	C 133 B 1102	Caprine	2nd phalanx	Final BA/EIA (1200–200 BC)	–19.47	8.02	13.82	38.71	3.3
BTC–KY–F78	Chap I	House floor	Cattle	Metacarpal	Final BA/EIA (1200–200 BC)	–19.68	7.70	17.12	46.77	3.2
BTC–KY–F79	Chap I	House floor	Caprine	Carpus/tarsus	Final BA/EIA (1200–200 BC)	–17.03	11.92	36.42	13.15	3.2
BTC–KY–F15	Chon–Alai	Rofot–Korgan, Kurgan 1	Caprine	Ulna	Final BA/EIA (1200–200 BC)	–18.33	6.03	17.49	44.85	3.0
BTC–KY–F30	Uch Kurbu	G–11, layer 9–8, dog burial	Dog	Metapodia	Final BA/EIA (1200–200 BC)	–19.14	8.96	10.90	32.13	3.4
BTC–KY–F31	Uch Kurbu	B2, L8, TTB	Caprine	Distal humerus	Final BA/EIA (1200–200 BC)	–19.40	7.66	18.83	51.00	3.2

BTC–KY–F32	Uch Kurbu	B2, L9, TTB	Cattle	Ulna	Final BA/EIA (1200–200 BC)	–16.03	7.76	16.76	45.66	3.2
BTC–KY–F33	Uch Kurbu	A3, L5, TTB	Caprine	Tibia	Final BA/EIA (1200–200 BC)	–19.34	6.88	11.47	32.55	3.3
BTC–KY–F54	Uch Kurbu	BA (Andronovo)	Big mammal (horse, cattle, etc.)	Bone fragment	Final BA/EIA (1200–200 BC)	–17.53	6.05	14.46	38.52	3.1
BTC–KY–F55	Uch Kurbu	BA (Andronovo)	Caprine	Bone fragment	Final BA/EIA (1200–200 BC)	–16.52	8.55	14.8	39.63	3.1
BTC–KY–F57	Uch Kurbu	BA (Andronovo)	Caprine	Bone fragment	Final BA/EIA (1200–200 BC)	–14.92	7.56	15.55	41.55	3.1
BTC–KY–F58	Uch Kurbu	BA (Andronovo)	Caprine	Bone fragment	Final BA/EIA (1200–200 BC)	–14.63	9.38	16.2	42.59	3.1
BTC–KY–F12	Aigyrzhal 1	Kurgan 20? 24?	Horse	Carpus/tarsus	Turkic–medieval (200 BC–AD 1700)	–20.64	5.50	17.40	44.88	3.0
BTC–KY–F13	Aigyrzhal 1	Ak–kiya, individual 2	Horse	Bone fragment	Turkic–medieval (200 BC–AD 1700)	–20.04	5.15	22.87	59.22	3.0
BTC–KY–F20	Aigyrzhal 1		Caprine	Bone fragment.	Turkic–medieval (200 BC–AD 1700)	–17.75	7.12	n/k	n/k	3.2
BTC–KY–F59	Aigyrzhal 1	Kurgan 24	Cattle	Distal tibia	Turkic–medieval (200 BC–AD 1700)	–20.46	5.24	20.13	51.73	3.0
BTC–KY–F60	Aigyrzhal 1	Kurgan 1	Horse	Skull	Turkic–medieval (200 BC–AD 1700)	–20.16	6.27	10.98	28.63	3.0
BTC–KY–F67	Aigyrzhal 2	Turkic (*c.* AD 4–7)	Caprine	Bone fragment	Turkic–medieval (200 BC–AD 1700)	–18.74	6.92	15.55	41.55	3.1
BTC–KY–F68	Aigyrzhal 3	Turkic (*c.* AD 4–7)	Medium mammal	Bone fragment	Turkic–medieval (200 BC–AD 1700)	–21.66	5.52	15.92	43.69	3.2
BTC–KY–F66	Kok–Sai	Hunic (AD 179–220)	Cattle	Bone fragment	Turkic–medieval (200 BC–AD 1700)	–16.27	7.74	41.16	15.3	3.1

BTC–KY–F69	Kok–Sai	En–2	Animal bone	Bone fragment	Turkic–medieval (200 BC–AD 1700)	–18.69	11.04	34.56	12.30	3.3
BTC–KY–F70	Kok–Sai	En–1	Caprine	Radius	Turkic–medieval (200 BC–AD 1700)	–18.69	10.99	27.20	9.57	3.3
BTC–KY–F71	Kok–Sai	Corral, 0.35m depth	Animal bone	Bone fragment	Turkic–medieval (200 BC–AD 1700)	–19.57	6.22	34.32	11.92	3.4
BTC–KY–F72	Kok–Sai	KY19.10F, Corral, 100mm depth	Caprine	Bone fragment	Turkic–medieval (200 BC–AD 1700)	–19.28	6.62	33.91	12.06	3.3
BTC–KY–F61	Kok–Tash	Proximal epiphysis	Horse	Tibia	Turkic–medieval (200 BC–AD 1700)	–19.91	5.62	13.16	37.31	3.3
BTC–KY–F62	Kok–Tash		Horse	Tibia	Turkic–medieval (200 BC–AD 1700)	–20.65	5.89	16.34	45.77	3.3
BTC–KY–F63	Kok–Tash	Metapodia UF	Caprine	Bone fragment	Turkic–medieval (200 BC–AD 1700)	–19.29	7.49	18.73	49.82	3.1

OSM B: Stable isotope analysis

Collagen extraction protocols and measurement of samples

The samples for stable isotope analysis were prepared in Bioarchaeology Research Centre at Vilnius University following the pre-treatment protocol outlined below:

- About 5g of bone was sampled
- The sampled bone was crushed to smaller pieces
- Samples were demineralised with 0.5 M HCl for 1–5 days
- After demineralisation, each sample was washed with distilled water until its pH level became 4–5
- pH 3 solution was added to each sample
- Samples in pH 3 solution were left in the 70° C for 24–48hr until they were fully gelatinised
- Samples were filtered
- Samples were frozen overnight at −30° C
- Samples were dried in a freeze-dryer
- 0.85–1.0 mg. was weighed from each sample, put into tin capsule and prepared for measuring

The samples were measured at the Center for Physical Scientific Research (Vilnius, Lithuania). An elemental analyser coupled to the isotope ratio mass spectrometer (EA-IRMS, Flash EA1112-Thermo V Advantage) via ConFlo III interface was used for the $\delta^{13}C$ and $\delta^{15}N$ analysis (see details in Garbaras *et al*. 2019). Carbon isotopic ratio measurements presented here are expressed relative to the Vienna Pee-Dee Belemnite (VPDB) standard, while the nitrogen isotopic ratio coincides with the air N2. The analytical precision and calibration of reference gas CO2 (for $\delta^{13}C$ measurements) to VPDB were evaluated by the repeated analysis of secondary reference material caffeine IAEA-600, and oil. The IAEA-600 standard was used for calibration of reference gases N2 ($\delta^{15}N$ measurements) to AIR (Table S2). Internal standards, flour and nicotinamide were used for tracing the analytical uncertainty (Table S3).

Table S2: Standard reference materials used for calibration of δ^{13}C relative to VPDB and δ^{15}N relative to AIR.

Standard	Material	Accepted δ^{13}C (‰, VPDB)	Accepted δ^{15}N (‰, AIR)
IAEA-600	Caffeine	−27.777±0.043	+1.0±0.2

Table S3: Standard reference materials used for to monitor internal accuracy and precision

Standard	Material	Mean $\delta^{13}C$ (‰, VPDB)	Mean $\delta^{15}N$ (‰, AIR)
IRM-1	Flour	−26.5	+3.2
IRM-2	Nicotinamide	−31.36	+2.07

Success rate

The preservation of collagen was measured by C:N ratio of 2.9–3.6 (DeNiro 1985). We originally acquired 86 human and 94 animal bone samples for the research. However, nine human and three animal samples failed the collagen extraction. All other samples were measured and showed good preservation of collagen.

Table S4. Summary of human isotopic values.

Site (n)	$\delta^{13}C$‰					$\delta^{15}N$‰				
	Min	**Max**	**Mean**	**SD**	**Median**	**Min**	**Max**	**Mean**	**SD**	**Median**
Early–Late Bronze Age (n = 46)	**–19.4**	**–12.3**	**–18.3**	**1.1**	**–18.6**	**10.0**	**16.9**	**12.0**	**1.2**	**11.8**
Aigyrzhal 1 (n = 7)	–18.8	–17.2	–18.2	0.6	–18.2	11.6	16.9	13.0	1.9	12.1
Aigyrzhal 2 (n = 8)	–18.8	–17.6	–18.2	0.5	–18.1	10.5	12.3	11.4	0.6	11.4
Aigyrzhal 3 (n = 21)	–19.4	–12.3	–18.6	1.5	–18.8	10.1	13.8	12.0	1.1	11.8
Chalchyk Bulak (n = 1)	–18.3	–18.3				12.5	12.5			
Kara-Tumshuk (n = 1)	–18.4	–18.4				11.9	11.9			
Kochkor burial grounds (n = 1)	–18.7	–18.7				12.7	12.7			
Kyrk-Sheyit (n = 3)	–19.2	–18.3	–18.7	0.4	–18.7	10.0	12.3	11.0	1.2	10.7
Shyldyrak (n = 3)	–18.3	–16.9	–17.5	0.8	–17.2	11.0	11.5	11.2	0.3	11.0
Chap II (n = 1)	–17.5	–17.5				12.7	12.7			
Final Bronze Age/Early Iron Age (n = 19)	**–18.7**	**–13.9**	**–17.3**	**1.40**	**–17.7**	**10.0**	**13.3**	**12.1**	**0.9**	**12.2**
Aygirzhal 1 (n = 4)	–18.5	–15.6	–17.5	1.30	–17.9	12.7	13.3	12.6	0.7	12.7
Aygirzhal 2 (n = 5)	–17.9	–14.5	–17.1	1.5	–17.7	12.1	13.1	12.5	0.4	12.5
Chap I (n = 3)	–18.7	–13.9	–17.0	2.7	–18.4	11.3	12.2	11.7	0.5	11.5
Chechen-Bulak (n = 1)	–16.9	–16.9				10.0	10.0			
Chon-Alai (n = 2)	–17.7	–17.2				10.7	11.4			

Mechet at-Bashi (n = 2)	–18.7	–18.1				12.9	12.9			
Uch-Kurbu (n = 1)	–17.0	–17.0				11.8	11.8			
Zhapyryk (n = 1)	–15.7	–15.7				12.1	12.1			
Turkic/Medieval (n = 13)	**–19.9**	**–15.3**	**–17.9**	**1.30**	**–18.3**	**11.7**	**17.3**	**13.3**	**1.5**	**12.9**
Aigyrzhal 1 (n = 12)	–19.9	–15.3	–18.0	1.30	–18.3	11.7	17.3	13.3	1.5	12.7
Kok-Tash (n = 1)	–16.9	–16.9				13.8	13.8			

Table S5. Summary of herbivore isotopic values.

Species (n)			**$\delta^{13}C$‰**					**$\delta^{15}N$‰**		
	Min	**Max**	**Mean**	**SD**	**Median**	**Min**	**Max**	**Mean**	**SD**	**Median**
Early–Late Bronze Age (n = 52)	**–21.1**	**–16.0**	**–19.2**	**1.0**	**–19.2**	**4.2**	**11.2**	**7.2**	**1.5**	**7.1**
Caprine (n = 22)	–20.2	–16.7	–19.0	0.7	–19.1	5.5	11.2	7.6	1.5	7.1
Cattle (n = 17)	–19.7	–16.0	–18.8	0.8	–19.0	6.6	9.7	7.7	0.8	7.5
Horse (n = 10)	–20.9	–17.1	–20.1	1.1	–20.5	4.2	7.8	5.8	1	5.6
Final Bronze Age/Early Iron Age (n = 15)	**–19.7**	**–14.6**	**–18.0**	**1.8**	**–189**	**6.0**	**11.9**	**7.8**	**1.4**	**7.6**
Caprine (n = 13)	–19.5	–14.6	–18.1	1.7	–18.9	6.0	11.9	7.8	1.5	7.5
Cattle (n = 2)	–19.7	–16.0				7.7	7.8			
Medieval (n = 12)	**–20.7**	**–16.3**	**–19.3**	**1.3**	**–19.6**	**5.2**	**11.0**	**6.7**	**1.6**	**6.4**
Caprine (n = 5)	–19.3	–17.8	–18.8	0.6	–18.7	6.6	11.0	7.8	1.8	7.1
Cattle (n = 2)	–20.5	–16.3				5.2	7.7			
Horse (n = 5)	–20.7	–19.9	–20.3	0.4	–20.2	5.2	6.3	5.7	0.4	5.6

Table S6. Previously published human isotopic values from Kyrgyzstan used for statistical comparisons.

Sample number	**Site**	**Context**	**Dating**	**$\delta^{13}C$**	**$\delta^{15}N$**	**C/N atomic**	**Reference**
N/A	Aygirdjal (Aigyrzhal)	K. 67	2203–2041 cal BC (3735±20 BP, PSUAMS–4607)	–17.69	11.91	3.2	Narasimhan *et al.* 2018
N/A	Aygirdjal (Aigyrzhal)	K. 67A	2114–1928 cal BC (3630±20 BP, PSUAMS–4750)	–18.14	11.44	3.1	Narasimhan *et al.* 2018
CGG_2_015973	Keden	Kurgan nr. K9 (individ. nr. 1)	168–83 BC	–17.06	13.63	3.2	de Barros Damgaard *et al.* 2018
CGG_2_015975	Keden	Kurgan nr. K45	356–285 BC	–18.27	11.68	3.2	de Barros Damgaard *et al.* 2018
CGG_2_015977	Keden	Kurgan nr. K53	361–349 BC	–16.91	12.24	3.2	de Barros Damgaard *et al.* 2018
CGG_2_015978	Keden	Kurgan nr. K60	403–434 BC	–17.50	12.51	3.2	de Barros Damgaard *et al.* 2018
CGG_2_015979	Keden	Kurgan nr. K71	453–446 BC	–17.84	14.03	3.3	de Barros Damgaard *et al.* 2018
CGG_2_015980	Keden	Kurgan nr. K70	265–271 BC	–17.61	11.88	3.2	de Barros Damgaard *et al.* 2018
CGG_2_015981	Keden	Kurgan nr. K65	89–74 BC	–17.34	12.98	3.2	de Barros Damgaard *et al.* 2018

CGG_2_015982	Keden	Kurgan nr. K63	159–132 BC	–17.53	12.74	3.2	de Barros Damgaard *et al.* 2018
CGG_2_015983	Baskya 1	Kurgan nr. 7	169–90 BC	–17.92	13.54	3.2	de Barros Damgaard *et al.* 2018
CGG_2_015984	Baskya 1	Kurgan nr. 3	166–89 BC	–17.43	13.41	3.2	de Barros Damgaard *et al.* 2018
CGG_2_015985	Baskya 1	Kurgan nr. 4	349–313 BC	–17.98	13.79	3.2	de Barros Damgaard *et al.* 2018
CGG_2_015989	Baskya 2	Kurgan nr. 1 (individ. 1, buried with individ. 2.),	AD 397–570	–15.10	11.80	3.2	de Barros Damgaard *et al.* 2018
CGG_2_015991	Baskya 2	Kurgan nr. 19	AD 382–433	–17.34	13.12	3.2	de Barros Damgaard *et al.* 2018
CGG_2_015992	Baskya 2	Kurgan nr. 10	AD 430–492	–15.55	12.61	3.2	de Barros Damgaard *et al.* 2018
CGG_2_015994	Baskya 2	Kurgan nr. 21	AD 557–615	–16.31	11.82	3.2	de Barros Damgaard *et al.* 2018
CGG_2_015995	Baskya 2	Kurgan nr. 25	AD 349–368	–15.76	12.36	3.2	de Barros Damgaard *et al.* 2018
CGG_2_015996	Baskya 2	Kurgan nr. 18 (child)	AD 60–143	–17.40	13.85	3.2	de Barros Damgaard *et al.* 2018
CGG_2_015997	Baskya 2	Kurgan nr. 20	AD 252–308	–14.10	12.50	3.2	de Barros Damgaard *et al.* 2018
CGG_2_015998	Baskya 2	Kurgan nr. 7	AD 264–274	–16.30	11.30	3.2	de Barros Damgaard *et al.* 2018
CGG_2_015999	Baskya 2	Kurgan nr. 2	AD 255–301	–15.10	12.80	3.2	de Barros Damgaard *et al.* 2018
CGG_2_016000	Baskya 2	Kurgan nr. 30 (child, buried together with another individual),	AD 385–435	–17.30	12.90	3.2	de Barros Damgaard *et al.* 2018
CGG_2_016006	Baskya 2	Kurgan nr. 5 (individ. 2 out of three individuals buried together, individual 3. is a child),	AD 257–297	–14.30	13.30	3.2	de Barros Damgaard *et al.* 2018
CGG_2_016007	Zhapyryk	Kurgan nr. 50	AD 177–190	–16.50	10.00	3.2	de Barros Damgaard *et al.* 2018
CGG_2_016008	Zhapyryk	Kurgan nr. 4	AD 83–177	–16.40	11.90	3.2	de Barros Damgaard *et al.* 2018
CGG_2_016010	Zhapyryk	Kurgan nr. 2	AD 170–194	–16.10	11.50	3.2	de Barros Damgaard *et al.* 2018
CGG_2_016011	Boz-Adyr	Kurgan nr. 16 (human (warrior) buried together with horse),	AD 424–474	–17.20	12.80	3.2	de Barros Damgaard *et al.* 2018
CGG_2_016012	Uch-Kurbu	Kurgan nr. 9	AD 259–281	–16.80	12.80	3.2	de Barros Damgaard *et al.* 2018
CGG_2_016014	Uch-Kurbu	Kurgan nr. 14 (individual 2.),	AD 61–144	–15.00	14.10	3.2	de Barros Damgaard *et al.* 2018
CGG_2_016015	Kyzyl-Too	Kurgan nr. 2	AD 1161–1255	–18.50	10.50	3.2	de Barros Damgaard *et al.* 2018
CGG_2_016016	Uch-Kurbu	Kurgan nr. 8	AD 255–300	–18.50	10.55	3.2	de Barros Damgaard *et al.* 2018
CGG_2_016017	Uch-Kurbu	Kurgan nr. 14 (individual 1.(child)),	AD 214–261	–16.30	12.60	3.2	de Barros Damgaard *et al.* 2018
CGG_2_016020	Uch-Kurbu	Kurgan nr. 1 / 2 (grav 2),		–15,90	16.20	3.1	de Barros Damgaard et al., 2018'

CGG_2_016021	Uch-Kurbu	Kurgan 1 / 4 (grav 4.),	AD 134–219	–16.50	12.11	3.1	de Barros Damgaard *et al.* 2018
CGG_2_016022	Boz-Adyr	Kurgan nr. 28	AD 1170–1171	–16.50	12.10	3.2	de Barros Damgaard *et al.* 2018
CGG_2_016024	Boz-Adyr	Kurgan nr. 36	AD 1156–1224	–18.00	10.60	3.2	de Barros Damgaard *et al.* 2018
CGG_2_016025	Boz-Adyr	Kurgan nr. 31	AD 1678–1696	–18.20	12.00	3.2	de Barros Damgaard *et al.* 2018
CGG_2_016026	Boz-Adyr	Kurgan nr. 38	AD 1029–1049	–18.70	13.30	3.1	de Barros Damgaard *et al.* 2018

Table S7. Information on the sites where the samples were collected. BA = Bronze Age; MBA = Middle Bronze Age; FBA = Final Bronze Age; EIA = Early Iron Age.

Site	No. of samples	Dating	Elevation
Aigyrzhal 1	23 humans, seven animals	BA–Medieval	2020m asl
Aigyrzhal 2	13 humans, 13 animals	BA-Medieval	2020m asl
Aigyrzhal 3	21 humans, two animals	BA–Medieval	2020m asl
Chalchyk-Bulak	one human	BA	3070m asl
Chap I	Three humans, seven animals	FBA/EIA	2000m asl
Chap II	One human, 33 animals	EBA–MBA	2000m asl
Chechen-Bulak	One human	EIA	1925m asl
Chon-Alai	Two humans, one animal	EIA	2680m asl
Kara-Tumshuk	One human, five animals	BA	1800m asl
Kochkor burial grounds	One human	BA	2200m asl
Kok-Sai	Five animals	Medieval	2000m asl
Kok-Tash mausoleum	One human, three animals	Medieval	1990m asl
Kyrk-Sheyit	Three humans	BA	2030m asl
Mechet at-Bashi	Two humans	EIA	2380m asl
Shyldyrak	Three humans	BA	990m asl
Uch-Kurbu	One human, eight animals	EBA–MBA	1720m asl
Zhapyryk	One human	EIA	2550m asl

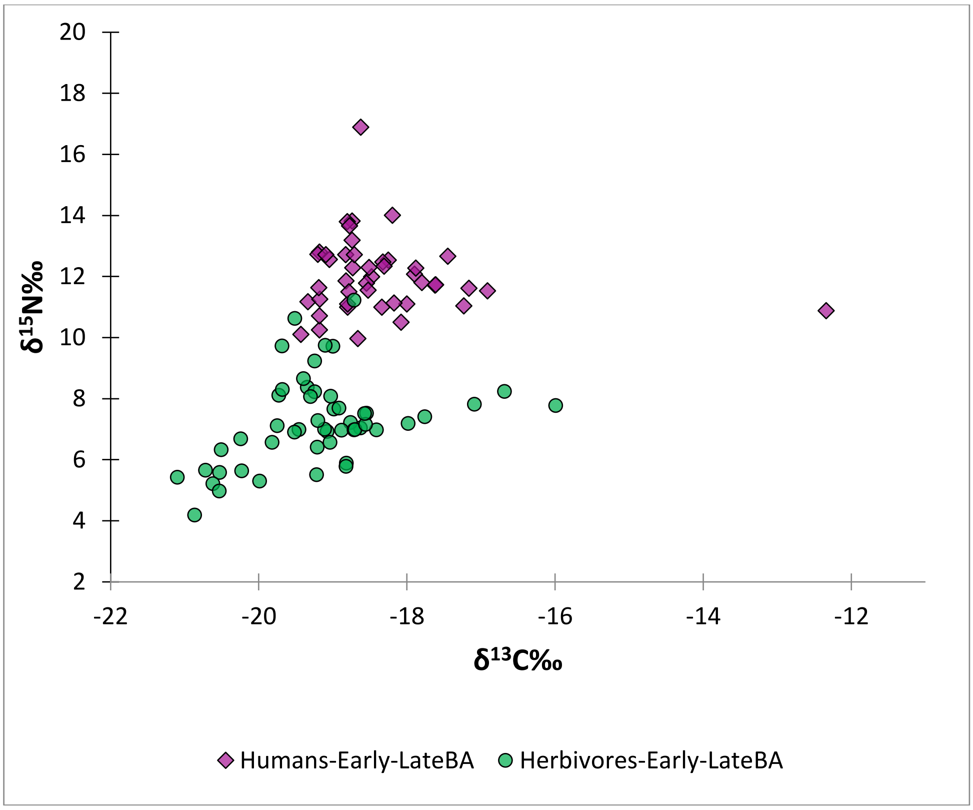

Figure S1. Scatter plot with Early–Late Bronze Age human and animal stable isotope analysis.

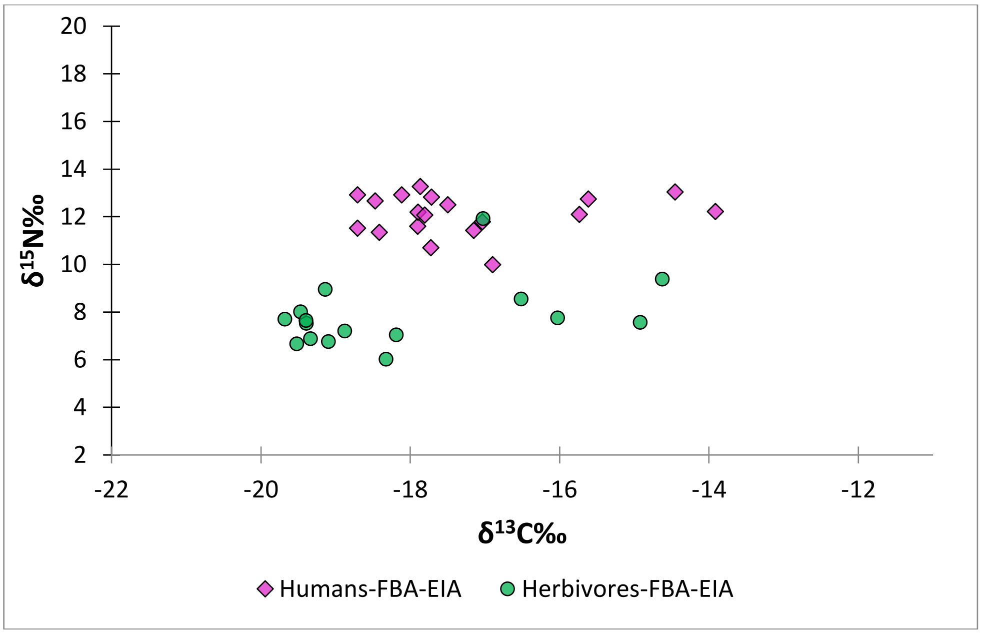

Figure S2. Scatter plot with Final Bronze Age/Early Iron Age human and animal stable isotope analysis.

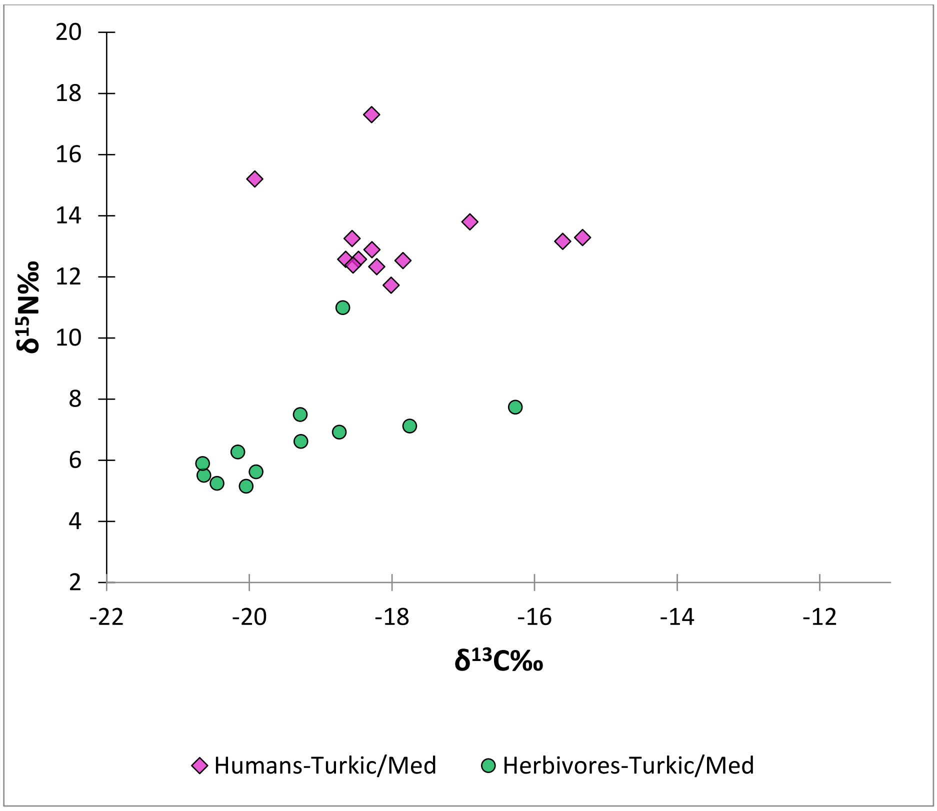

Figure S3. Scatter plot with Turkic–Medieval human and animal stable isotope analysis.

Table S8. Results of the ^{14}C dating of human and animal bone collagen samples from Kyrgyzstan.

^{14}C Lab number	BTC lab number	Site	Context	Material type	^{14}C Age	±	δ^{13}C	Calibrated age BC/AD
FTMC-MP17-4	BTC-KY-H13	Aigyrzhal 1	Kurgan 1	human collagen	1493	35	−15.3	444–648
FTMC-MP17-5	BTC-KY-H12	Aigyrzhal 1	Kurgan 7. burial 1	human collagen	1724	37	−15.6	247–411
UBA-23655	BTC-KY-F20	Aigyrzhal 1	Ritual pit	caprine bone collagen	3345	32	−17.8	1736–1533
UBA-27672	BTC-KY-H25	Aigyrzhal 2		human collagen	3899	35	−17.8	2471–223
UBA–27673	BTC–KY–H26	Aigyrzhal 2	cairn	human collagen	3913	32	−18.8	2475–2289
UBA–27674	BTC–KY–H28	Aigyrzhal 2	stone cyst	human collagen	3526	38	−18.8	1959–1742
UBA–27675	BTC–KY–H32	Aigyrzhal 2	Kurgan 33	human collagen	2522	29	−17.5	790–544
UBA–27676	BTC–KY–H33	Aigyrzhal 2	Kurgan 10	human collagen	2352	29	−17.9	517–382
FTMC–MP17–2	BTC–KY–H48	Aigyrzhal 3	Kurgan 139	human collagen	3856	36	−12.3	2460–2204
UBA–27677	BTC–KY–H37	Aigyrzhal 3		human collagen	3160	33	−18.0	1504–1320
FTMC–MP17–3	BTC–KY–H60	Chap I	Human burial	human collagen	2742	35	−13.9	979–811
FTMC–YL92–1	BTC–KY–F45	Chap II		cattle bone collagen	3760	29	−16.0	2287–2041

UBA–41510	BTC–KY–H66	Kara–Tumshuk	Child's burial	juvenile human collagen	3257	29	−18.4	1612–1448

OSM C: collagen peptide mass fingerprinting

Preparation and measurement of samples

The ZooMS analysis presented here was carried out at the palaeoproteomics lab of the Department of Life Sciences and Systems Biology (University of Torino) using the collagen extracted at Centre for Bioarchaeology Research (see collagen extraction protocol in the Supplementary Material–B). First of all, the lyophilised collagen extracts were dissolved in 200μL HPLC–grade water. 20μL of each aliquot was subsampled and transferred to separate eppendorfs (LoBind), evaporated using a centrifugal evaporator (Eppendorf concentrator plus) and resuspended in 100μL 50mM ammonium bicarbonate (ABC) solution. Following this, samples were reduced with 1M DL–dithiothreitol (Sigma, Canada) for 1h at 65°C and alkylated with 0.5M iodoacetamide (Sigma, USA) at room temperature in the dark for 45min. Digestion was carried out using trypsin (Promega, VP111, proteomics grade) at 37°C for ~18hrs (overnight). Digestion was stopped with 10% TFA (to a final concentration of 0.1%). Digested peptides were purified and concentrated using C18 solid–phase extraction tips (Pierce zip–tip) according to established protocols.

0.5μL aliquots of peptide solution were mixed with 0.5μL of α–cyano–4–hydroxycinnamic acid (HCCA) matrix solution (1%, prepared in 50% acetonitrile/0.1%trifluoracetic acid (*v/v*)) and spotted on a MTB Biotarget 96 MALDI stainless steel plate. Each sample was spotted in duplicate and analyzed in manual mode on a bench–top Microflex LRF MALDI–TOF mass spectrometer (Bruker Daltonics, Germany) at the Department of Clinical and Biological Sciences (Ospedale San Luigi Gonzaga), University of Turin. Samples were analyzed in reflector mode, using the following parameter settings: ion source 1 18.96 kV; ion source 2 16.02 kV; lens voltage 9.05 kV, reflector 20.01 kV, laser power 22%. The spectrum collected for each sample resulted from the sum of 1000 laser shots. Mass range was 800–4000 *m/z* and peptide masses below 650 Da were suppressed. The peptide calibration standard (#8206195, Bruker Daltonics, Germany), a mixture of seven peptides (Angiotensin II *m/z*=1046.541, Angiotensin I *m/z* = 1296.685, Substance_P *m/z* = 1347.735, Bombesin *m/z* = 1619.822, ACTH (1–17 clip) *m/z* = 2093.086, ACTH (18–39 clip) *m/z* = 2465.198 and Somatostatin *m/z* = 3147.471) was used for external mass calibration to maximise mass accuracy. The spectra were exported as text files and further analysed using the open access Mmass tool (Niedermeyer & Strohalm 2012). All of the resulting spectra were processed by performing baseline correction, smoothing; peak picking was performed selecting an S/N threshold ≥6. Internal mass calibration was carried out using trypsin, matrix and keratin *m/z* values.

Results and taxonomic identification

The analysis and taxonomic identification of collagen samples was successfully obtained for majority of the samples. All identifications were based on the previously published markers (Buckley *et al*. 2014, 2018; Welker *et al*. 2016; Desmond *et al*. 2018).

Table S9. The table lists all the samples that were analysed in this study, obtained species IDs and peptide markers (*m/z*; Deam* notes deamidated peptide markers).

Sample	**No**	**Identification**	**Peptide markers (*m/z*)**
BTC–KY–F34	1	*Capra* sp.	A – 1180.7; B – 1427.7; D – 2131.0; E – 2793.2 (Deam*); F – 2883.3; G' – 3093.5
BTC–KY–F34	2	*Capra* sp.	A – 1180.7; B – 1427.7; D – 2131.0; E – 2792.3; F – 2883.4; G' – 3093.5
BTC–KY–F35	1	*Bos/Bison*	A – 1192.6; A' – 1208.7; B – 1427.7; D – 2131.0; F – 2853.4; G – 2018.4 (Deam*); G' – 3033.5
BTC–KY–F35	2	*Bos/Bison*	A – 1192.7; A' – 1208.8; B – 1427.8; D – 2131.0; E – 2793.2 (Deam*); F – 2853.4; G – 3017.4; G' – 3034.5 (Deam*)
BTC–KY–F36	1	*Bos/Bison*	A – 1192.7; A' – 1208.8; B – 1427.7; D – 2131.0; E – 2793.2 (Deam*); F – 2853.4; G – 3017.4; G' – 3033.5
BTC–KY–F36	2	*Bos/Bison*	A – 1192.7; A' – 1208.8; B – 1427.7; D – 2131.0; E – 2793.2 (Deam*); F – 2853.4; G – 3017.6; G' – 3034.6 (Deam*)
BTC–KY–F37	1	Unresolved	B – 1427.7; D – 2131.0; E – 2793.2 (Deam*); F – 2883.4; G – 3017.5; G' – 3033.5
BTC–KY–F37	2	*Ovis* sp. or *Rupicapra* sp. but not *Capra* sp.	A – 1180.8; B – 1427.7; C – 1580.8; D – 2131.0; E – 2792.2; F – 2883.3; G – 3017.4; G' – 3033.6
BTC–KY–F38	1	*Bos/Bison*	A' – 1208.7; B – 1427.7; C – 1580.8; D – 2131.1; F – 2853.5; G – 3018.3 (Deam*); G' – 3034.6 (Deam*)
BTC–KY–F38	2	*Bos/Bison*	A' – 1208.7; B – 1427.7; C – 1580.8; D – 2131.0; F – 2853.3; G – 3018.4 (Deam*); G' – 3034.4 (Deam*)
BTC–KY–F39	1	*Bos/Bison*	A' – 1208.7; B – 1427.7; C – 1580.8; D – 2131.0; E – 2793.2 (Deam*); F – 2853.3; G – 3018.4 (Deam*); G' – 3034.4 (Deam*)
BTC–KY–F39	2	*Bos/Bison*	A' – 1208.6; B – 1427.7; D – 2131.0; E – 2793.3 (Deam*); F – 2853.4; G – 3018.5 (Deam*); G' – 3033.6

BTC–KY–F40	1	*Ovis* sp. or *Rupicapra* sp. but not *Capra* sp.	A – 1196.7; B – 1427.7; C – 1580.7; D – 2131.0; E – 2792.2; F – 2883.3; G – 3017.5; G' – 3033.5
BTC–KY–F40	2	*Ovis* sp. or *Rupicapra* sp. but not *Capra* sp.	A – 1196.7; B – 1427.7; C – 1580.7; D – 2131.0; E – 2792.3; F – 2883.4; G – 3017.5; G' – 3033.5
BTC–KY–F41	1	*Bos/Bison*	A' – 1208.6; B – 1427.7; D – 2131.0; E – 2793.2 (Deam*); F – 2853.4; G – 3017.4; G’ – 3033.5
BTC–KY–F41	2	*Bos/Bison*	A' – 1208.7; B – 1427.7; D – 2131.0; E – 2793.3 (Deam*); F – 2853.4; G – 3018.4 (Deam*); G’ – 3033.5
BTC–KY–F42	1	*Bos/Bison*	A – 1192.7; A' – 1208.7; B – 1427.7; D – 2131.1; F – 2853.5; G – 3018.5 (Deam*); G’ – 3034.6 (Deam*)
BTC–KY–F42	2	*Bos/Bison*	A' – 1208.7; B – 1427.7; C – 1580.7; D – 2131.0; E – 2793.3 (Deam*); F – 2853.4; G – 3018.5 (Deam*); G’ – 3033.6
BTC–KY–F43	1	*Ovis* sp. or *Rupicapra* sp. or *Ovibos* sp. but not *Capra* sp.	B – 1427.7; C – 1580.7; D – 2131.1; F – 2883.4; G – 3018.5 (Deam*); G' – 3033.5
BTC–KY–F43	2	*Ovis* sp. or *Rupicapra* sp. or *Ovibos* sp. but not *Capra* sp.	B – 1427.7; D – 2131.0; F – 2883.4; G – 3018.4 (Deam*); G' – 3033.5
BTC–KY–F44	1	*Ovis* sp. or *Rupicapra* sp. or *Ovibos* sp. but not *Capra* sp.	B – 1427.7; C – 1580.7; D – 2131.0; E – 2793.2 (Deam*); F – 2883.3; G – 3018.4 (Deam*); G' – 3034.5
BTC–KY–F44	2	*Ovis* sp. or *Rupicapra* sp. or *Ovibos* sp. but not *Capra* sp.	B – 1427.7; C – 1580.7; D – 2131.0; E – 2792.3; F – 2883.4; G – 3017.5; G' – 3033.5
BTC–KY–F45	1	*Bos/Bison*	A' – 1208.7; B – 1427.7; C – 1580.7; D – 2131.0; E – 2793.2 (Deam*); F – 2853.3; G – 3017.5; G’ – 3033.5
BTC–KY–F45	2	*Bos/Bison*	A' – 1208.7; B – 1427.7; C – 1580.7; D – 2131.0; E – 2793.2 (Deam*); F – 2853.4; G – 3017.4; G’ – 3033.5
BTC–KY–F46	1	*Ovis* sp. or *Rupicapra* sp. or *Ovibos* sp. but not *Capra* sp.	B – 1427.7; C – 1580.7; D – 2131.0; E – 2793.2 (Deam*); F – 2883.3; G – 3017.6; G' – 3034.5 (Deam*)
BTC–KY–F46	2	*Ovis* sp. or *Rupicapra* sp. or *Ovibos* sp. but not *Capra* sp.	A – 1196.5; B – 1427.7; C – 1580.7; D – 2131.0; E – 2792.2; F – 2883.4; G – 3017.5; G' – 3033.5
BTC–KY–F47	1	*Bos/Bison*	A' – 1208.6; B – 1427.7; D – 2131.0; E – 2793.2 (Deam*); F – 2853.3; G – 3017.4; G’ – 3033.5
BTC–KY–F47	2	*Bos/Bison*	A' – 1208.7; B – 1427.7; C – 1580.8; D – 2131.0; E – 2793.3 (Deam*); F – 2853.4; G – 3017.5; G’ – 3033.5
BTC–KY–F48	1	*Bos/Bison*	A' – 1208.7; B – 1427.7; D – 2131.0; E – 2793.3 (Deam*); F – 2853.4; G – 3018.5 (Deam*); G’ – 3033.6
BTC–KY–F48	2	*Bos/Bison*	A' – 1208.7; B – 1427.7; C – 1580.7; D – 2131.0; E – 2793.3 (Deam*); F – 2853.4; G – 3017.5; G’ – 3033.6
BTC–KY–F49	1	*Bos/Bison*	A' – 1208.7; B – 1427.7; D – 2131.0; E – 2792.3; F – 2853.3; G – 3017.5; G’ – 3033.6

BTC–KY–F49	2	*Bos/Bison*	A' – 1208.7; B – 1427.7; D – 2131.0; E – 2792.3; F – 2853.4; G – 3017.5; G’ – 3033.6
BTC–KY–F50	1	*Bos/Bison*	A' – 1208.7; B – 1427.7; C – 1580.7; D – 2131.0; E – 2792.3; F – 2853.4; F' – 2869.4; G – 3017.5; G’ – 3033.5
BTC–KY–F50	2	*Bos/Bison*	B – 1427.7; D – 2131.0; E – 2793.2 (Deam*); F – 2853.4; G – 3017.5; G’ – 3033.6
BTC–KY–F51	1	*Bos/Bison*	A' – 1208.7; B – 1427.7; C – 1580.7; D – 2131.0; E – 2793.2 (Deam*); F – 2853.3; G – 3017.5; G’ – 3033.5
BTC–KY–F51	2	*Bos/Bison*	A' – 1208.7; B – 1427.7; D – 2131.0; E – 2793.3 (Deam*); F – 2853.4; G – 3017.5; G’ – 3033.5

Table S10. Results of ZooMS analysis and isotopic measurements of indeterminate skeletal fragments from Chap II.

Lab. Code	Context	Result	$\delta^{13}C$	$\delta^{15}N$	C/N_{at}
BTC–KY–F34	C2.3D	*Capra*	–19.4	8.4	3.2
BTC–KY–F35	C2.3D	*Bos*	–18.8	7.2	3.2
BTC–KY–F36	C2.3D	*Bos*	–19.0	6.6	3.2
BTC–KY–F37	C2.3B	*Ovis* or *Rupicapra*	–19.5	7.0	3.2
BTC–KY–F38	C2.4.1G	*Bos*	–19.4	8.7	3.2
BTC–KY–F39	C2.4.1G	*Bos*	–19.1	7.0	3.2
BTC–KY–F40	C2.4.1G	*Ovis* or *Rupicapra*	–19.0	7.7	3.2
BTC–KY–F41	C2.4.1G	*Bos*	–18.9	7.0	3.2
BTC–KY–F42	C2.4.1G	*Bos*	–18.9	7.7	3.2
BTC–KY–F43	C2.4.1G	*Ovis* or *Rupicapra*	–19.7	8.1	3.2
BTC–KY–F44	C2.2C	*Ovis*, *Rupicapra* or *Ovibos*	–19.1	6.9	3.2
BTC–KY–F45	C2.2C	*Bos*	–16.0	7.8	3.2
BTC–KY–F46	C2.1F	*Ovis, Rupicapra or Ovibos*	–18.8	5.8	3.2
BTC–KY–F47	C2.1F	*Bos*	–18.6	7.5	3.2
BTC–KY–F48	C2.1F	*Bos*	–18.7	7.0	3.2
BTC–KY–F49	C2.1F	*Bos*	–19.2	7.3	3.4
BTC–KY–F50	C2.1F	*Bos*	–18.7	7.0	3.2
BTC–KY–F51	C2.1F	*Bos*	–19.0	8.1	3.3

Spectra images

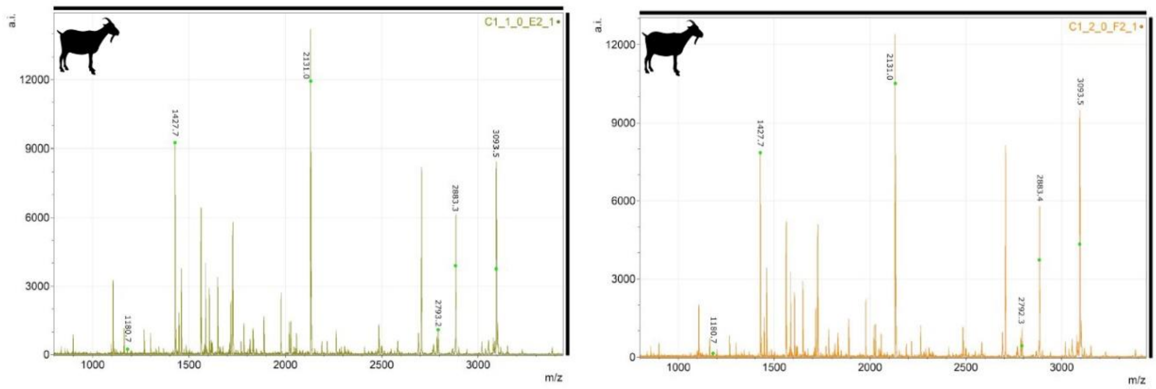

Figure S4. Spectrum image of sample BTC–KY–F34 (left) and BTC–KY–F34 duplicate (right).

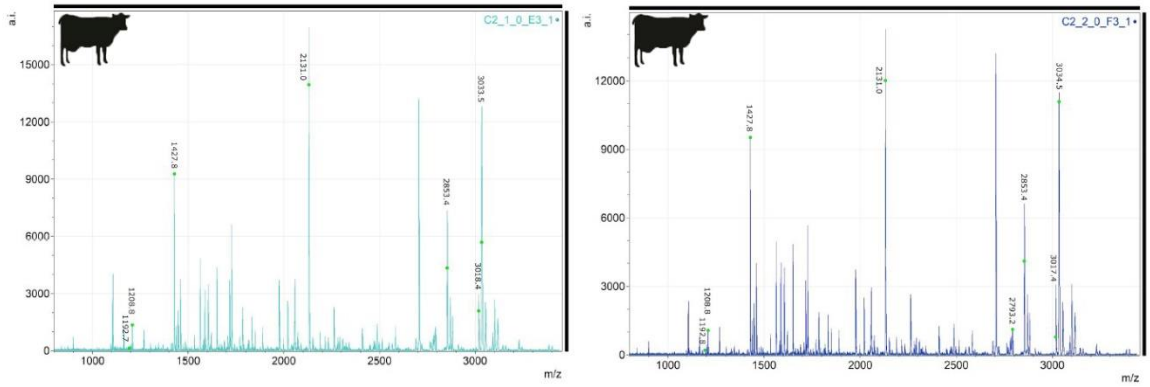

Figure S5. Spectrum image of sample BTC–KY–F35 (left) and BTC–KY–F35 duplicate (right).

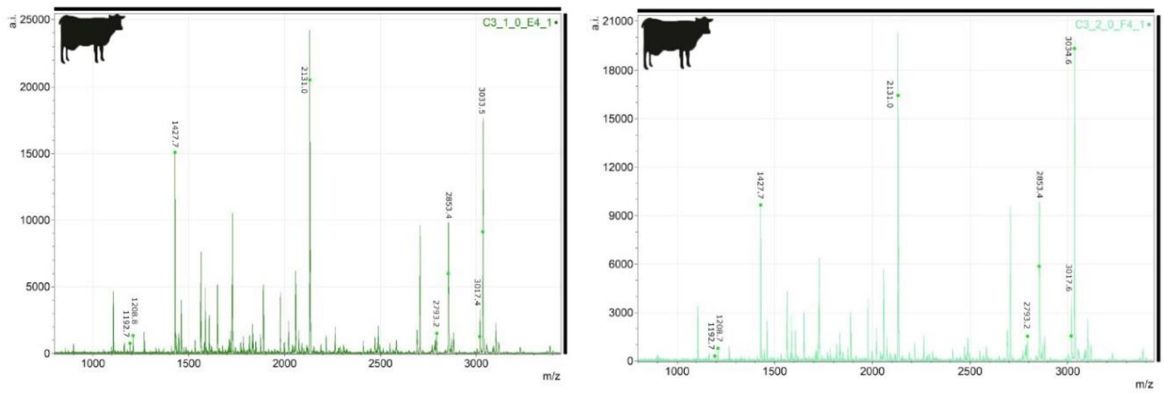

Figure S6. Spectrum image of sample BTC–KY–F36(left) and BTC–KY–F36 duplicate (right).

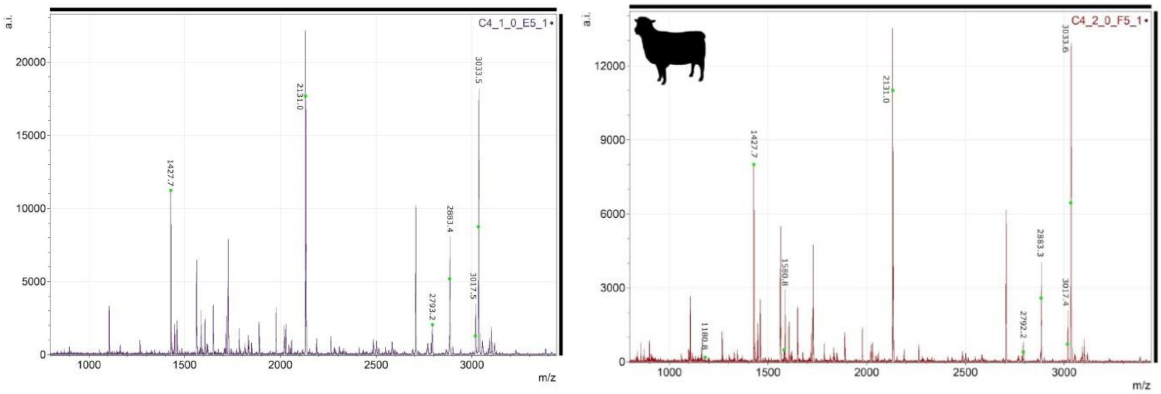

Figure S6. Spectrum image of sample BTC–KY–F37 (left) and BTC–KY–F37 duplicate (right). Sample BTC–KY–F37 (left) did not give enough marker peaks, therefore identification was not possible.

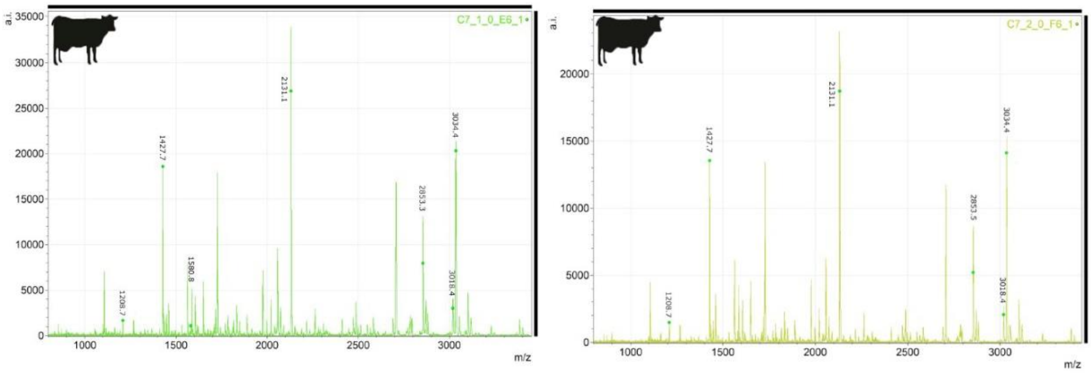

Figure S7. Spectrum image of sample BTC–KY–F38 (left) and BTC–KY–F38 duplicate (right).

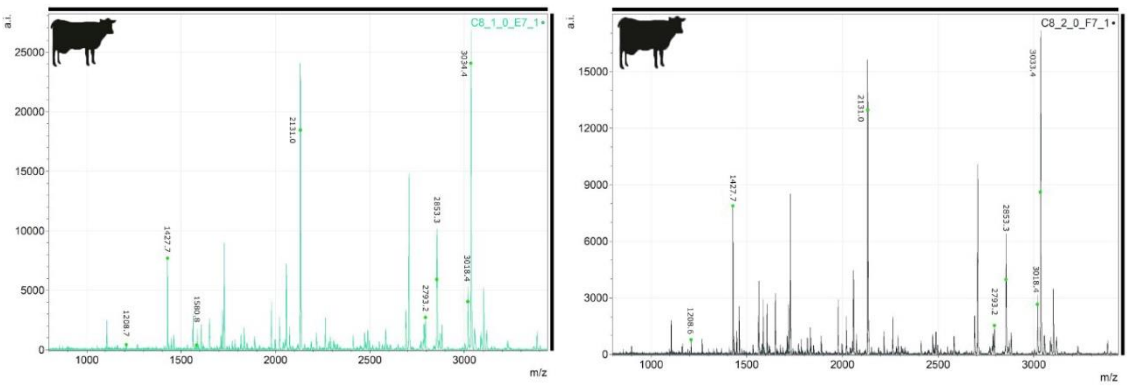

Figure S8. Spectrum image of sample BTC–KY–F39 (left) and BTC–KY–F39 duplicate (right).

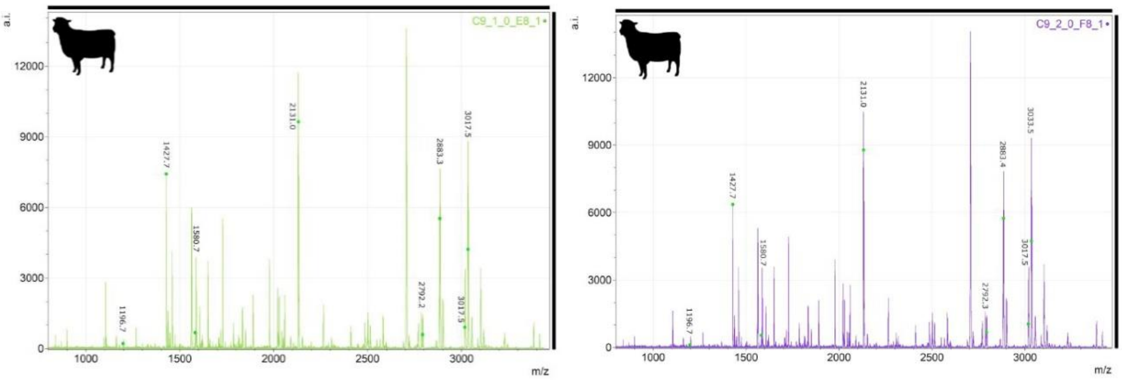

Figure S9. Spectrum image of sample BTC–KY–F40 (left) and BTC–KY–F40 duplicate (right).

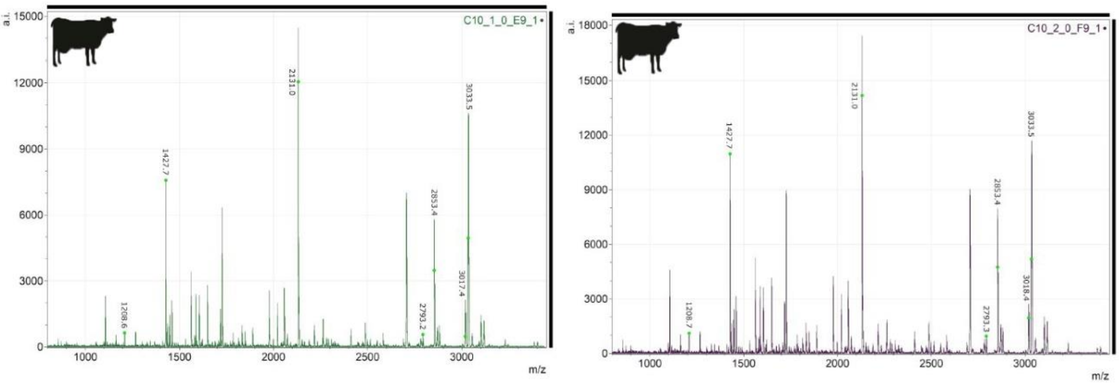

Figure S10. Spectrum image of sample BTC–KY–F41 (left) and BTC–KY–F41 duplicate (right).

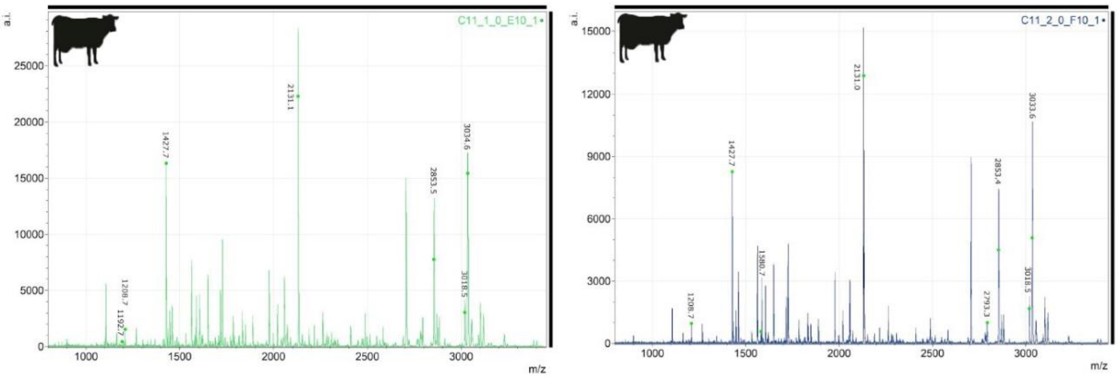

Figure S11. Spectrum image of sample BTC–KY–F42 (left) and BTC–KY–F42 duplicate (right).

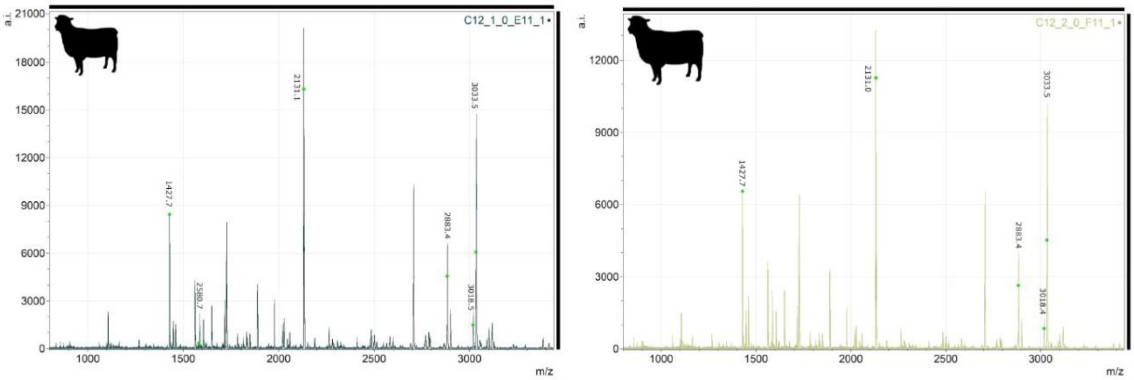

Figure S12. Spectrum image of sample BTC–KY–F43 (left) and BTC–KY–F43 duplicate (right).

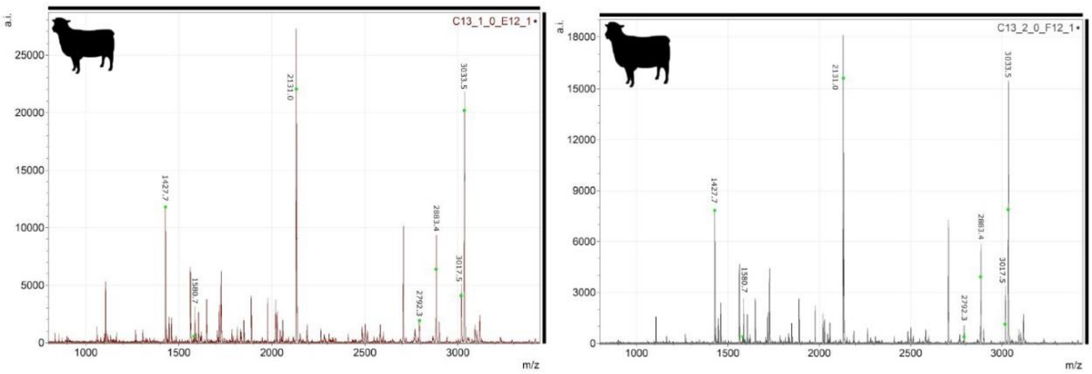

Figure S13. Spectrum image of sample BTC–KY–F44 (left) and BTC–KY–F44 duplicate (right).

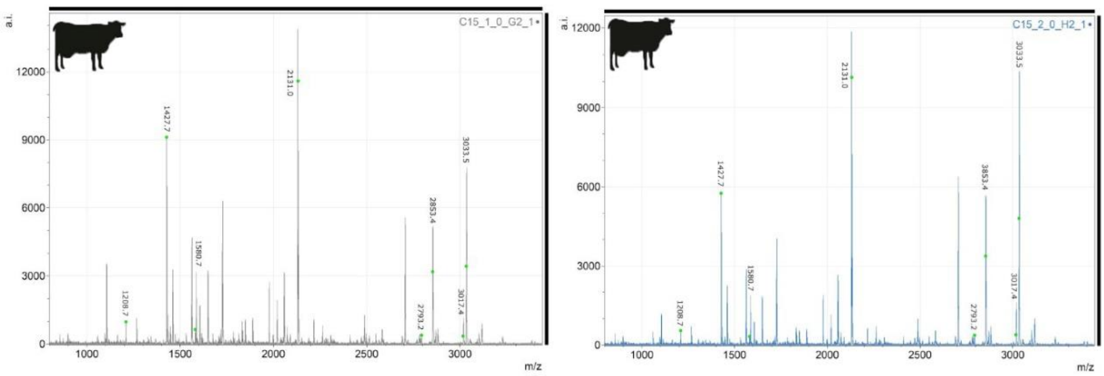

Figure S14. Spectrum image of sample BTC–KY–F45 (left) and BTC–KY–F45 duplicate (right).

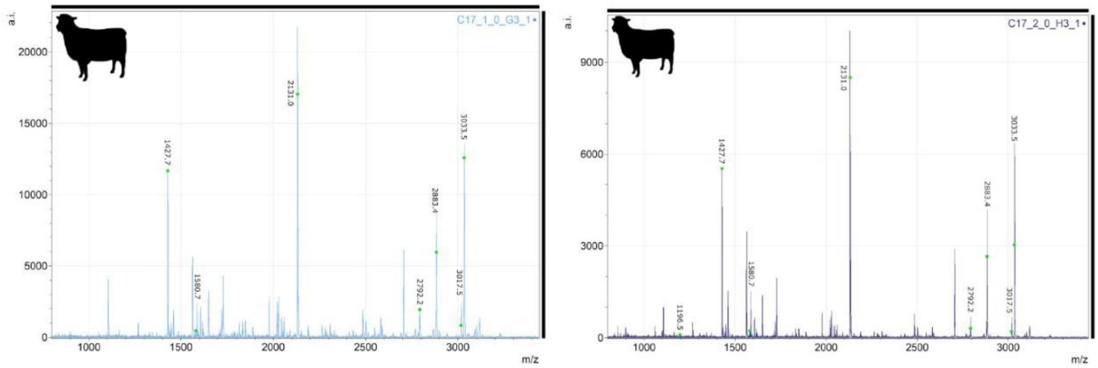

Figure S15. Spectrum image of sample BTC–KY–F46 (left) and BTC–KY–F46 duplicate (right).

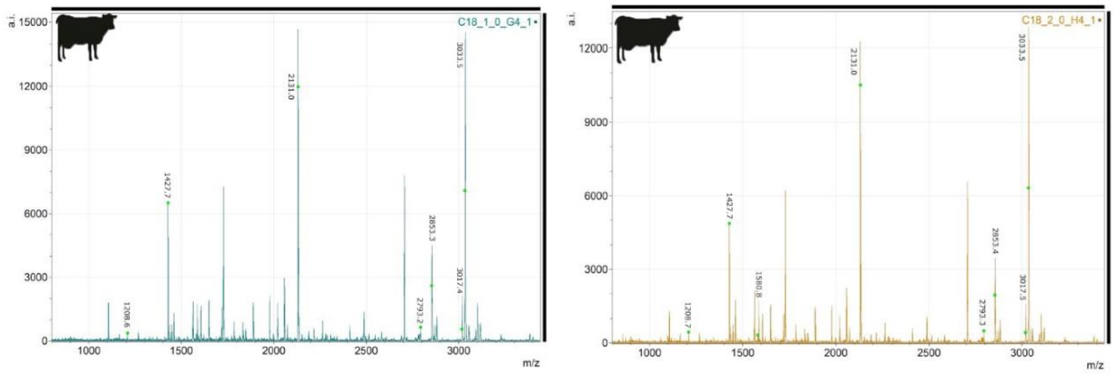

Figure S16. Spectrum image of sample BTC–KY–F47 (left) and BTC–KY–F47 duplicate (right).

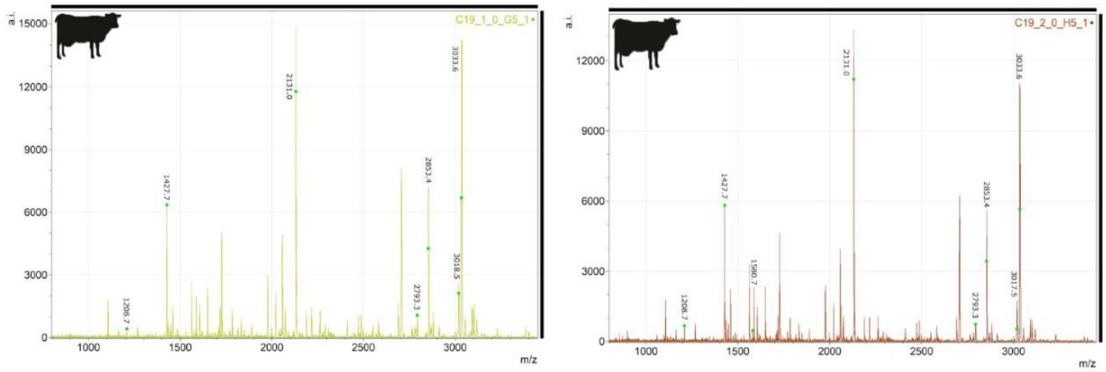

Figure S17. Spectrum image of sample BTC–KY–F48 (left) and BTC–KY–F48 duplicate (right).

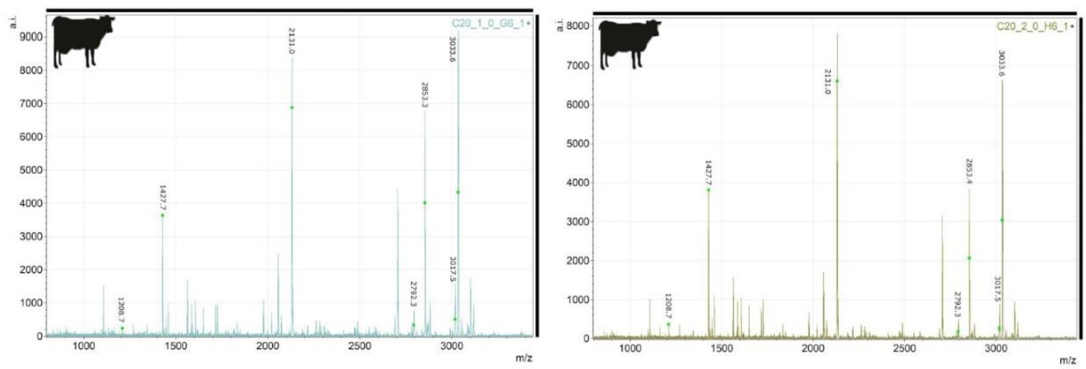

Figure S18. Spectrum image of sample BTC–KY–F49 (left) and BTC–KY–F49 duplicate (right).

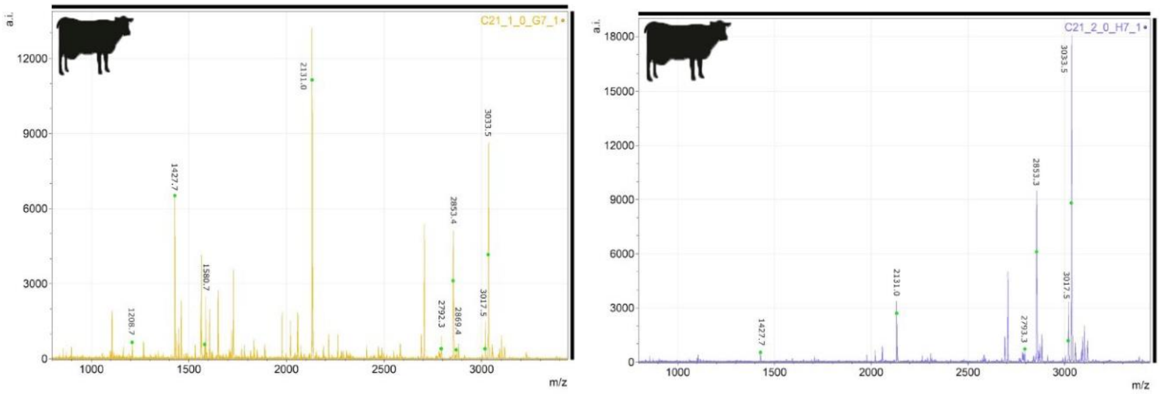

Figure S19. Spectrum image of sample BTC–KY–F50 (left) and BTC–KY–F50 duplicate (right).

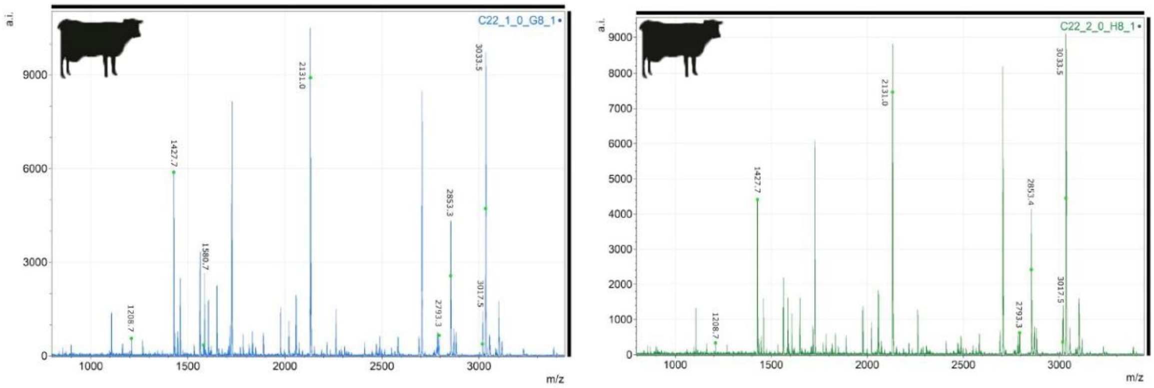

Figure S20. Spectrum image of sample BTC–KY–F51 (left) and BTC–KY–F51 duplicate (right).

References

BUCKLEY, M. *et al*. 2014. Species identification of archaeological marine mammals using collagen fingerprinting. *Journal of Archaeological Science* 41: 631–41. https://doi.org/10.1016/j.jas.2013.08.021

– 2018. Species identification of voles and lemmings from Late Pleistocene deposits in Pin Hole Cave (Creswell Crags, UK) using collagen fingerprinting. *Quaternary International* 483: 83–89. https://doi.org/10.1016/j.quaint.2018.03.015

DE BARROS DAMGAARD, P. *et al*. 2018. The first horse herders and the impact of Early Bronze Age steppe expansions into Asia. *Science* 360: eaar7711. https://doi.org/10.1126/science.aar7711

DENIRO, M.J. 1985. Postmortem preservation and alteration of in vivo bone collagen isotope ratios in relation to palaeodietary reconstruction. *Nature* 317: 806. https://doi.org/10.1038/317806a0

DESMOND, A. *et al*. 2018. ZooMS identification of bone tools from the North African Later Stone Age. *Journal of Archaeological Science* 98: 149–57. https://doi.org/10.1016/j.jas.2018.08.012

GARBARAS, A. *et al*. 2019. Seasonal variation in stable isotope ratios of cow milk in Vilnius region, Lithuania. *Animals* 9: 69. https://doi.org/10.1038/317806a0

NARASIMHAN, V.M. *et al*. 2018. The genomic formation of South and Central Asia. *bioRxiv* 292581.

NIEDERMEYER, T.H. & M. STROHALM. 2012. mMass as a software tool for the annotation of cyclic peptide tandem mass spectra. *PLoS ONE* 7: e44913. https://doi.org/10.1371/journal.pone.0044913

WELKER, F. *et al*. 2016. Palaeoproteomic evidence identifies archaic hominins associated with the Châtelperronian at the Grotte du Renne. *Proceedings of the National Academy of Sciences of the USA* 11340: 11162–67. https://doi.org/10.1073/pnas.1605834113

OSM D: list of references for Figure 6.

Locations with millet evidence across Central Asia and Kashmir: 1) Aigyrzhal–3; 2) Chap I,II; 3) Uch–Kurbu; 4) Chechen–Bulak; 5) Kara–Tumshuk; 6) Alatau; 7) Kamenka; 8) Kargaly–1; 9) Kyzylasker; 10) Ornek; 11) Kyzyl Bulak; 12) Turgen–2; 13) Karatuma; 14) Karkara; 15) Serektas; 16) Khatau–1; 17) Shatyrkul'; 18) Shokpar; 19) Oi–Dzhailau 7–8; 20) Kainarbulak–1; 21) Shymkent; 22) Kaitpas; 23) Burgulyuk; 24) Babish Mulla–7; 25) Chirik Rabat; 26) Geoktchik Tepe; 27) Taksai–2; 28) Myrzhyk–6; 29) Tegiszhol; 30) Kurgan Borli; 31) Bozshakol; 32) Karazhartas; 33) Akbeit; 34) Karashoky; 35) Koitas; 36) Taldy–2; 37) Tasyrbai; 38) Kent; 39) Kyzyl; 40) Aktogai; 41) Kazakh Mys; 42) Karatobe; 43) Zevakinskyi; 44) Firsovo–11; 45) Afanasyeva Gora; 46) Karasuk III; 47) Uibat V; 48) Ai–Dai; 49) Aymyrlyg; 50) Begash; 51) Pethpuran Teng; 52) Kokel;53) Shorthugai; 54) Gonur; 55) Ojakly; 56) 1211/19; 57) Tasbas; 58) Tongtian cave; 59) Dingildzhe; 60) Farmstead 641; 61) Tahirbaj Tepe; 62) Kyzyltepa; 63) Novy–Kumak–2; 64) Tuzusai; 65) Taldy–Bulak–2; 66) Tseganka 8; 67) Dali; 68) Abylai; 69) Ushlep–5; 70) Maima–1; 71) Kazylgan; 72) Nargas Tepe.

Previously published data used for the map was collected from: Abdulganeyev (1997); Akbulatov (1999); Ananyevskaya *et al*. (2018, 2020); Andrianov (1969); Bakkels (2003);

Beisenov *et al*. (2019); Bocherens *et al*. (2006); Frachetti *et al*. (2010); Hermes *et al*. (2019); Lightfoot *et al*. (2015); Motuzaite Matuzeviciute *et al.* (2015, 2016, 2018, 2020); Murphy *et al.* (2013); Nesbitt (1994); Ramaroli *et al.* (2010); Spengler *et al.* (2013, 2014, 2017); Svyatko & Beisenov (2017); Svyatko *et al.* (2013); Tolstov & Vaynberg (1967); Vainshtein (1980); Vorobyeva (1973); Vorobyeva & Gertman (1991); Wu *et al.* (2015); Yatoo *et al.* (2020); Zhou *et al.* (2020).

ABDULGANEYEV, M.T. 1997. O nalichii zemledeliya u naseleniya lesostepnogo i predgornogo altaya v epokhu zheleza, in Y.F. Kiryushin & A.A. Tishkin (ed.) *Sotsialno–ekonomicheskiye struktury drevnikh obschestv zapadnoi sibiri: materialy vserossyiskoi nauchnoi konferencii*: 138–41. Barnaul: Altaiskyi gosudarstvennyi universitet.

AKBULATOV, I. M. 1999. *Ekonomika rannih kochevnikov Yuzhnogo Urala (VII v. do n. e.–IV v. n. e.).* Ufa: Nacionalyi Muzei Respubliki Bashkortostan.

ANANYEVSKAYA, E. *et al*. 2017. Early indicators to C_4 plant consumption in central Kazakhstan during the Final Bronze Age and Early Iron Age based on stable isotope analysis of human and animal bone collagen. *Archaeological Research in Asia* 15: 157–73. https://doi.org/10.1016/j.ara.2017.12.002

– 2020. The effect of animal herding practices on the diversity of human stable isotope values in North Central Asia. *Journal of Archaeological Science: Reports* 34: 102615. https://doi.org/10.1016/j.jasrep.2020.102615.

ANDRIANOV, B.V. 1969. *Drevniye orositel'niye sistemy Priaralya (v svyazi s istoriei vozniknoveniya i razvitiya oroshaemogo zemledeliya).* Moscow: Nauka. Glavnaya redakciya vostochnoi literatury.

BOCHERENS, H. *et al*. 2006. Stable isotope evidence for palaeodiets in southern Turkmenistan during the Historical period and Iron Age. *Journal of Archaeological Science* 33: 253–64. https://doi.org/10.1016/j.jas.2005.07.010

BAKKELS, C.C. 2003. The contents of ceramic vessels in the Bactria–Margiana Archaeological Complex, Turkmenistan. *Electronic Journal of Vedic Studies* 9: 49–52.

BEISENOV, A.Z. *et al*. 2020. New isotopic data on the diet of the Saka period population from central Kazakhstan. *Povolzhskaya Arheologiya* 3: 208–18. https://doi.org/10.24852/pa2020.3.33.208.218

FRACHETTI, M.D., R.N. SPENGLER, G.J. FRITZ & A.N. MAR’YASHEV. 2010. Earliest direct evidence for broomcorn millet and wheat in the central Eurasian steppe region. *Antiquity* 84: 993–1010. https://doi.org/10.1017/S0003598X0006703X

HERMES, T.R. *et al*. 2019. Early integration of pastoralism and millet cultivation in Bronze Age Eurasia. *Proceedings of the Royal Society B: Biological Sciences* 286: 20191273. https://doi.org/10.1098/rspb.2019.1273

LIGHTFOOT, E. *et al*. 2015. How 'pastoral' is pastoralism? Dietary diversity in Bronze Age communities in the central Kazakhstan steppes. *Archaeometry* 57: 232–49. https://doi.org/10.1111/arcm.12123

MOTUZAITE MATUZEVICIUTE, G. *et al*. 2015. The extent of cereal cultivation among the Bronze Age to Turkic period societies of Kazakhstan determined using stable isotope analysis of bone collagen. *Journal of Archaeological Science* 59: 23–34. https://doi.org/10.1016/j.jas.2015.03.029

– 2016. Climatic or dietary change? Stable isotope analysis of Neolithic–Bronze Age populations from the Upper Ob and Tobol River Basins. *The Holocene* 26**:** 1711–21. https://doi.org/10.1177/0959683616646843

– 2018. The effect of geographical margins on cereal grain size variation: case study for highlands of Kyrgyzstan. *Journal of Archaeological Science: Reports* 20: 400–10. https://doi.org/10.1016/j.jasrep.2018.04.037

– 2020. High–altitude agro–pastoralism in the Kyrgyz Tien Shan: new excavations of the Chap farmstead (1065–825 cal BC). *Journal of Field Archaeology* 45: 29–45. https://doi.org/10.1080/00934690.2019.1672128.

MURPHY, E.M. *et al*. Iron Age pastoral nomadism and agriculture in the eastern Eurasian steppe: implications from dental palaeopathology and stable carbon and nitrogen isotopes. *Journal of Archaeological Science* 40: 2547–60. https://doi.org/10.1016/j.jas.2012.09.038

NESBITT, M. 1994. Archaeobotanical research in the Merv Oasis. International Merv project, preliminary report on the second season (1993). Unpublished field report, Iran.

RAMAROLI, V. *et al*. 2010. The Chehr Abad salt men and the isotopic ecology of humans in ancient Iran. *American Journal of Physical Anthropology* 143: 343–54. ttps://doi.org/10.1002/ajpa.21314

SPENGLER, R.N., C. CHANG & P.A. TOURTELLOTTE. 2013. Agricultural production in the Central Asian mountains: Tuzusai, Kazakhstan (410–150 BC). *Journal of Field Archaeology* 38**:** 68–85. https://doi.org/10.1179/0093469012Z.00000000037

SPENGLER, R.N. *et al*. 2014. Agriculturalists and pastoralists: Bronze Age economy of the Murghab alluvial fan, southern Central Asia. *Vegetation History and Archaeobotany* 23: 805–20. https://doi.org/10.1007/s00334–014–0448–0

– 2017. Linking agriculture and exchange to social developments of the Central Asian Iron Age. *Journal of Anthropological Archaeology* 48: 295–308. https://doi.org/10.1016/j.jaa.2017.09.002

SVYATKO, S.V. & A.Z. BEISENOV. 2017. Perviye izotopniye danniye o diete naseleniya tasmolinskoi kultury. *Samarskyi Nauchnyi Vestnik* 6: 223–27. https://doi.org/10.17816/snv201763223

SVYATKO, S.V. *et al*. 2013. Stable isotope dietary analysis of prehistoric populations from the Minusinsk Basin, southern Siberia, Russia: a new chronological framework for the introduction of millet to the eastern Eurasian steppe. *Journal of Archaeological Science* 40: 3936–45. https://doi.org/10.1016/j.jas.2013.05.005

TOLSTOV, S.P. & B.L. VAYNBERG. 1967. K*oi–Krylgan–kala: Pamyatnik Kultury Drevnego Khorezma IV veka do n.e.–IV veka n.e*. Moscow: Nauka.

VAINSHTEIN, S. 1980. *Nomads of South Siberia: the pastoral economies of Tuva*. Cambridge University Press: Cambridge.

VOROBYEVA, M.G. 1973. *Dingild'zhe: Usad'ba Serediny I Tysyacheletiya do n. e. v Drevnem Khorezme*. Moscow: Nauka.

VOROBYEVA, M.G. & N.A. GERTMAN. 1991. Raskopki dvukh usadeb vtoroi poloviny I tysyacheletiya n.e. v Djanbaskalinskom oazise, in G.M. Vinogradov (ed.) *Noviye otkrytiya v Priaralye 1*: 34–71. Moscow: Nauka.

WU, X., N.F. MILLER & P. CRABTREE. 2015. Agro–pastoral strategies and food production on the Achaemenid frontier in Central Asia: a case study of Kyzyltepa in southern Uzbekistan. *Iran* 53**:** 93–117. https://doi.org/10.1080/05786967.2015.11834752

YATOO, M.A. *et al*. 2020. New evidence from the Kashmir Valley indicates the adoption of East and West Asian crops in the western Himalayas by 4400 years ago. *Quaternary Science Advances* 2: 100011. https://doi.org/10.1016/j.qsa.2020.100011

ZHOU, X. *et al*. 2020. 5200–year–old cereal grains from the eastern Altai Mountains redate the trans–Eurasian crop exchange. *Nature Plants* 6: 78–87. https://doi.org/10.1038/s41477–019–0581–y